Leaflet No.

The Republic of the Union of Myanmar
Ministry of Natural Resources and Environmental Conservation

Growth Potential of the Mathislewald under Climate Change

Nyi Thu Ta, Range Officer, Forest Department
Dr. Julian Frey, Forest Sciences, European Forestry
Prof. Dr. René Orth, Forest Sciences, European Forestry

March, 2026

Contents

Growth Potential of the Mathislewald under Climate Change

Nyi Thuta, Range Officer

Forest Department

Abstract

Forests of Central Europe are undergoing rapid transformation under climate change, with altered growth patterns, shifting species composition, and increasing disturbance risks. This thesis investigates the growth potential of the Mathislewald forest, a montane mixed forest in the southern Black Forest of Germany, using the individual-based and process-oriented forest model iLand. The study focuses on a 1.69 ha research plot initialized with two high-resolution datasets: (i) a terrestrial laser scanning (TLS)-derived remote sensing (RS) inventory, and (ii) a complementary ground-truth (GT) field inventory. These were combined with site-specific soil properties, snag pools, and dynamically downscaled climate projections for RCP2.6, RCP4.5, and RCP8.5 for the period 2025–2100. One hundred replicates per scenario were conducted to quantify variability in growth, productivity, structural development, species dynamics, and mortality. Results show that climate forcing is the primary driver of forest trajectories. Under RCP4.5, moderate warming and CO_2 fertilization stimulated productivity and growth increments, while RCP8.5 produced strong early gains but led to summer stress, reduced vitality, and suppressed increments later in the century. Structural stocks such as basal area, biomass, and stem volume increased across all scenarios but plateaued earlier under RCP8.5. Species composition shifted consistently, with Picea abies declining and Fagus sylvatica and Abies alba gaining dominance. Diversity increased modestly under moderate scenarios, but RCP8.5 produced unstable dynamics and higher mortality. Seasonal analyses further highlighted spring productivity gains offset by summer collapse under strong forcing. RS initialization generated denser stands with smaller trees, whereas GT initialization produced taller but less crowded canopies. Despite these differences, both approaches converged on similar directional responses, confirming the reliability of TLS-derived inventories for process-based modeling. Overall, the results illustrate both risks and opportunities for Central European montane forests. Under moderate scenarios, productivity and resilience can be maintained through adaptive management that promotes structural diversity and drought-tolerant species. Under high-emission trajectories, however, forests risk entering fragile states with declining vitality and unstable carbon dynamics. By bridging remote sensing and process-based modeling, this thesis provides methodological advances and practical guidance for developing climate-adaptive forest management strategies.

Keywords: *Climate change impacts, forest growth modeling, iLand, remote sensing (TLS), species dynamics and productivity.*

ရာသီဥတုပြောင်းလဲမှုအောက်တွင် မာသစ်လ်ဝါလ်ဒ် သစ်တော၏ ကြီးထွားနိုင်စွမ်း အလားအလာ

ညီသုတ၊ တောအုပ်ကြီး
သစ်တောဦးစီးဌာန

စာတမ်းအကျဉ်း

ဗဟိုဥရောပဒေသရှိ သစ်တောများသည် ရာသီဥတုပြောင်းလဲမှုကြောင့် သစ်ပင်ကြီးထွားမှု၊ မျိုးစိတ်ဖွဲ့စည်းပုံနှင့် သစ်တောတည်ငြိမ်မှုတို့တွင် အပြောင်းအလဲများ ကြုံတွေ့လျက်ရှိသည်။ ဤ သုတေသနသည် ဂျာမနီနိုင်ငံ တောင်ပိုင်း Black Forest ဒေသရှိ Mathislewald တောင်တန်း ပေါင်းစပ်သစ်တော၏ ကြီးထွားနိုင်စွမ်းကို ပုဂ္ဂိုလ်ရေးအခြေခံနှင့် လုပ်ငန်းစဉ်အခြေခံသစ်တောမော်ဒယ်iLandကို အသုံးပြု၍ လေ့လာသုံးသပ်ခြင်းဖြစ်ပါသည်။ လေ့လာ မှုကို အကျယ်အဝန်း ၁.၆၉ ဟက်တာရှိ သုတေသနကွက်တစ်ခုအပေါ် အခြေခံ၍ ဆောင်ရွက် ခဲ့ပြီး၊ မြေပြင်လေဆာစကန်နင်းမှ ရရှိလာသော သစ်တောအပင်အချက်အလက် နှင့် မြေပြင် အခြေခံ စစ်ဆေးမှတ်တမ်း သစ်တောအပင်အခက်အလက်တို့ကို ပေါင်းစပ် အသုံးပြုခဲ့ပါသည်။ ထိုအချက်အလက်များကို နေရာ ဒေသအလိုက် မြေဆီလွှာအင်္ဂါရပ်များနှင့် ၂၀၂၅ မှ ၂၁၀၀ အထိ ကာလ အတွက် RCP2.6၊ RCP4.5 နှင့် RCP8.5 ရာသီဥတုအခြေအနေများ အောက်တွင် ခန့်မှန်းထားသော ရာသီဥတုအချက်အလက်များ နှင့်ပေါင်းစပ်၍ မော်ဒယ်သတ်မှတ်ခဲ့သည်။ အခြေအနေ တစ်ခုချင်းစီအတွက် အကြိမ်ကြိမ် စမ်းသပ်မှု ၁၀၀ကြိမ် ဆောင်ရွက်ခဲ့သည်။ ရလဒ်များအရ သစ်တောဖွံ့ဖြိုးတိုးတက်မှုကို အဓိကသတ်မှတ် ပေးသည့်အချက်မှာ ရာသီဥတုအခြေအနေ ဖြစ်ကြောင်းတွေ့ရှိရသည်။ RCP4.5 အောက်တွင် အပူချိန်အလယ်အလတ် မြင့်တက်မှုကြောင့် ထုတ်လုပ်နိုင်စွမ်းနှင့် ကြီးထွားမှု တိုးတက်လာသည်။ RCP8.5 အောက်တွင် အစောပိုင်း ကာလ၌ ကြီးထွားမှု တိုးတက်ခဲ့သော်လည်း နောက်ပိုင်းတွင် နွေရာသီအပူနှင့် ရေရှားပါးမှု ဖိအားများကြောင့် သစ်တောကျန်းမာရေးနှင့် ကြီးထွားမှု လျော့နည်းလာသည်။ မျိုးစိတ်ဖွဲ့စည်းပုံအရ Picea abies သည် လျော့နည်းသွားပြီး Fagus sylvatica နှင့် Abies alba တို့၏ အရေးပါမှု တိုးလာသည်။ စတင်ဒေတာ အချက်အလက် မတူကွဲပြားသော်လည်း သစ်တော၏ အနာဂတ်တုံ့ပြန်မှု လမ်းကြောင်းများသည် တူညီသည့် ဦးတည်ချက်ကို ပြသခဲ့ပြီး အဝေးထိန်းအာရုံခံလေဆာ စကန်နင်းမှရရှိသော သစ်တောစာရင်းများကို လုပ်ငန်းစဉ် အခြေခံမော်ဒယ်များတွင် ယုံကြည် စိတ်ချစွာ အသုံးပြုနိုင်ကြောင်းကို ပြသနေသည်။ ဤလေ့လာမှု၏ ရလဒ်များသည် အလယ် အလတ် ရာသီဥတု အခြေအနေများ အောက်တွင် အလိုက်သင့် သစ်တော စီမံခန့်ခွဲမှုများ ဖြင့်ထုတ်လုပ်နိုင်စွမ်းနှင့် သစ်တောခံနိုင်ရည်ကို ထိန်းသိမ်းနိုင်ကြောင်း ဖော်ပြနေပြီး၊ အပြင်း အထန်ရာသီဥတု ပြောင်းလဲမှုအောက်တွင်မူ သစ်တောများ၏ တည်ငြိမ်မှုလျော့နည်းနိုင်ကြောင်း တွေ့ရှိခဲ့ပါသည်။

Growth potential of the Mathislewald under climate change

1 Introduction

1.1 Background

Forests are critical components of the Earth system, providing essential ecosystem services including carbon storage, water regulation, soil stabilization, and biodiversity support (Bonan 2008; Pan et al. 2011; Global Forest Resources Assessment 2020). Globally, forests remove approximately 3.2 gigatonnes of carbon (~11.7 $GtCO_2$) annually and cover about 31% of the Earth's land surface, supporting more than 80% of terrestrial species (Le Quéré et al. 2018; Global Forest Resources Assessment 2020). Beyond carbon sequestration, forests regulate climate through biophysical feedbacks such as albedo modification and evapotranspiration, influencing regional and global climate systems (Anderson et al. 2011; Bonan 2008).

In Europe, forests hold strong socio-economic and cultural significance (Spiecker 2003), yet they are increasingly affected by anthropogenic climate change. Rising temperatures, altered precipitation patterns, and more frequent extreme events—including droughts, heatwaves, and storms—are driving shifts in species composition, productivity, phenology, and disturbance regimes (Allen et al. 2010; Seidl et al. 2014; Intergovernmental Panel On Climate Change (IPCC) 2023). These impacts are particularly pronounced in managed forests where species selection may not align with emerging climatic conditions (Brang et al. 2014).

Monospecific stands dominated by *Picea abies* are especially vulnerable, raising concerns about long-term resilience (Seidl et al. 2017). Species differ in their physiological responses to climatic stress, and future conditions are expected to favor more drought-tolerant taxa while reducing the competitiveness of traditionally dominant species such as *Picea abies*, *Fagus sylvatica*, and *Pinus sylvestris* (Hanewinkel et al. 2012; Hlásny et al. 2014).

The Mathislewald forest in the southern Black Forest, Germany, provides a representative case for assessing climate change impacts on montane mixed forests. A 1.69 ha research plot was initialized using high-resolution terrestrial laser scanning (TLS) data and a complementary ground-truth inventory, enabling precise application of the iLand model. By integrating tree-level inventory data with site-specific soil and climate inputs, this study projects future trajectories of growth, biomass accumulation, and species composition under alternative climate scenarios. Although plot-specific, the results offer broader insights into the dynamics and adaptation potential of Central European montane forests under climate change.

1.2 Research Problem

The increasing frequency and intensity of climate-related disturbances, including drought-induced dieback, bark beetle outbreaks, and windthrow, have exposed the vulnerability of many European forests (Senf and Seidl 2020; Hartmann et al. 2018). In Central Europe, these interacting stressors threaten forest structure and ecological functioning (Seidl et al. 2017; Ehbrecht et al. 2021). Prolonged droughts have caused widespread mortality in sensitive species such as *Picea abies*, raising concerns about the long-term viability of dominant tree species under changing climatic conditions (Allen et al. 2010; Pretzsch et al. 2018).Modeling has become an essential tool for projecting forest dynamics and informing management decisions. However, many empirical or statistical models rely on relationships that may not remain valid under novel climate regimes (Morin et al. 2018) and often fail to capture emergent processes, species interactions, and ecological feedbacks (Bugmann et al. 2019).

Process-based forest landscape models, such as iLand (individual-based forest landscape and disturbance model), simulate physiological and ecological mechanisms underlying tree growth, mortality, and regeneration, making them suitable for long-term scenario analysis (Seidl et al. 2012; Thom et al. 2019; Morales et al. 2007). Despite their advantages, these models require detailed initialization data on forest structure and site conditions, which can limit their broader application (Seidl et al. 2012; Bychkov and Popova 2023).Recent advances in remote sensing, particularly terrestrial laser scanning (TLS), provide high-resolution, spatially explicit tree-level information that can support process-based model initialization (Liang et al. 2016; Calders et al. 2020). TLS-derived inventories align well with the input requirements of individual-based models such as iLand (Seidl et al. 2012). In this context, the present study integrates TLS-based remote sensing (RS) and ground-truth (GT) inventory data to simulate forest development in the Mathislewald under RCP2.6, RCP4.5, and RCP8.5 scenarios from 2025–2100 (IPCC 2014).

2 Objectives

This study aims to assess the growth potential, structural development, and species dynamics of the Mathislewald forest under projected climate conditions using the iLand model. In doing so, it integrates remote sensing (RS)-based forest inventory data with process-based ecological modeling. In this thesis, the RS dataset refers specifically to terrestrial laser scanning (TLS)-derived individual tree data, which is complemented by a ground-truth (GT) field inventory. The specific objectives are –

1. To initialize the iLand model for a 1.69 ha research plot in the Mathislewald using RS (TLS)-derived individual tree data, a complementary GT inventory, and site-specific environmental inputs such as soil, climate, and topography.
2. To simulate forest development trajectories from 2025 to 2100 under three Representative Concentration Pathways (RCP2.6, RCP4.5, RCP8.5).
3. To quantify temporal changes in forest productivity and structural indicators, including increments, net primary productivity (NPP), total biomass, basal area, and leaf area index (LAI).
4. To assess shifts in species composition, dominance, and diversity under alternative climate scenarios, with an emphasis on identifying potentially vulnerable and resilient species.
5. To compare outcomes between RS and GT initialization and discuss their implications for scenario interpretation and adaptive forest management.

3. Methods and Manuscript setup

3.1 Study Area

The study was conducted in the Mathislewald forest in the Southern Black Forest, Baden-Württemberg, Germany (431902 E, 5303900 N; ETRS89 / UTM Zone 32N). The region is classified as temperate oceanic (Cfb) under the topography-corrected Köppen–Geiger system (Beck et al. 2018).

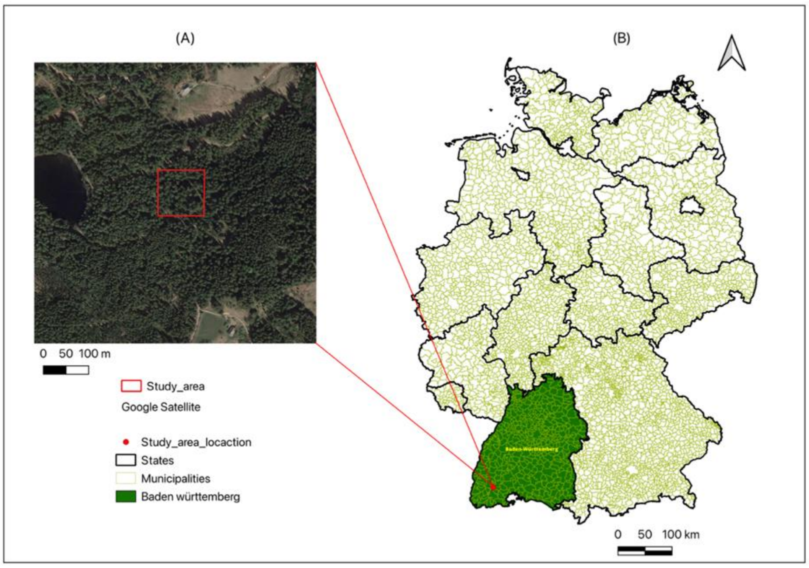

Figure 1 Location of the study area. (A) Detailed view of the Mathislewald forest with the study plot outlined in red. (B) The Mathislewald forest (red dot) within Baden-Württemberg, Germany.

Elevation ranges from approximately 900 to 1,100 m a.s.l., corresponding to the montane vegetation belt of Central Europe (Leuschner and Ellenberg 2017). The site's elevation and mixed conifer–broadleaf composition make it suitable for studying climate–growth relationships in Central European mixed forests (Bolte et al. 2009; Schuldt et al. 2020). The climate is characterized by cool summers, persistent winter snow cover, and high precipitation, supporting stands dominated by *Fagus sylvatica*, *Abies alba*, and *Picea abies* (Leuschner and Ellenberg 2017).

Long-term records from the Feldberg/Schwarzwald station (1,493 m a.s.l.) indicate a mean annual temperature of 3.9 °C and mean annual precipitation of 1,642 mm (DWD 2025). These cool and humid conditions favor high biomass accumulation and shade-tolerant, late-successional species (Leuschner and Ellenberg 2017).

Soils are mainly dystric cambisols and podzols developed over granitic and gneissic bedrock (Prietzel 2001). They are acidic, nutrient-poor, and moderately deep, with low base saturation despite partial recovery in recent decades (Prietzel et al. 2016; Meesenburg et al. 2019). Mineral weathering and mycorrhizal activity partly compensate for nutrient limitations (Heisner et al. 2004). These edaphic conditions favor stress-tolerant montane species such as *Fagus sylvatica*, *Abies alba*, and *Picea abies* (Leuschner and Ellenberg 2017).

3.2 Climate Data and Processing

Climate forcing for the iLand simulations was derived from dynamically downscaled datasets (1951–2100) based on the ICHEC-EC-EARTH global climate model under RCP2.6, RCP4.5, and RCP8.5 (Moss et al. 2010; van Vuuren et al. 2011). Regionalisation was performed using the CLMcom-CCLM4-8-17 model within the EURO-CORDEX framework (Jacob et al. 2014; Kotlarski et al. 2014).

To account for local topographic effects, datasets were corrected using lapse-rate-based elevation adjustments and climate cluster assignment following Dollinger et al. (2025). Daily lapse rates were applied with a high-resolution DEM to adjust grid-cell values to the elevation of the Mathislewald plot (~1,000 m a.s.l.), reducing biases from coarse topography and improving representation of snow and precipitation processes (Giorgi et al. 2009). A cluster-based approach linked the site to the most representative regional climate type (Huth et al. 2008; Dollinger et al. 2024). Because the study area covers only 1.69 ha, a single cluster dataset was used without additional statistical bias correction.

Separate SQLite climate files were generated for each RCP and integrated via the <climate> section of the iLand XML. Daily inputs included minimum and maximum temperature, precipitation, vapour pressure deficit (VPD), and shortwave radiation for both historical (1951–2024) and scenario periods (2025–2100). Atmospheric CO_2 concentrations were aligned with each RCP using the <co2pathway> setting, ensuring consistency between climate forcing and physiological responses defined in the <CO2Response> module (Seidl et al. 2012). This multi-scenario framework enables robust assessment of forest sensitivity to emission-driven climate change and projected meteorological variability.

3.3 Stand Grid Design

The simulation landscape was structured as a 21 × 21 stand grid (441 stands), with each stand measuring 100 × 100 m (1 ha), resulting in a total simulated area of 441 ha (2,100 × 2,100 m). The <standGrid> configuration referenced an ASCII raster generated in R with 10 m resolution to ensure accurate spatial mapping within iLand (Seidl et al. 2012).

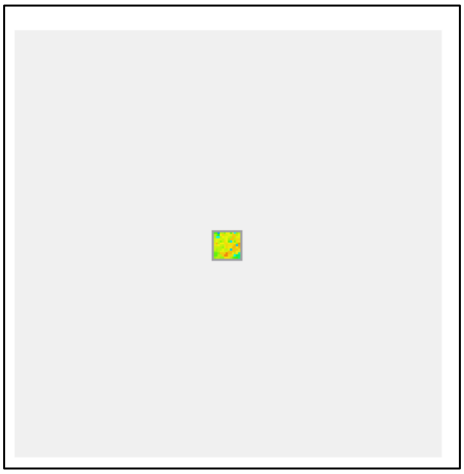

Figure 2 iLand stand grid for the Mathislewald plot, with the central initialized stand (colored) surrounded by forested outside pixels (grey) to reduce edge effects.

The central empirical plot (approximately 123 × 129 m) occupied one stand and contained the full individual-tree inventory (Section 3.4). The surrounding 440 stands were designated as Forested Outside Pixels (FOPs; stand value = –2), functioning as virtual forest buffers. In iLand, FOPs provide external light competition, seed input, and edge effects without contributing to output statistics (Seidl et al. 2012).

This configuration minimized edge effects that can bias growth and regeneration in small simulation domains (Seidl et al. 2012). The FOP buffer exceeded maximum seed dispersal distance, ensuring realistic seed input from a continuous surrounding forest matrix. Such buffering stabilizes stand-scale simulations by maintaining external competition and wind exposure conditions (Seidl et al. 2012).

The 10 m raster resolution aligns with disturbance and canopy modules, including wind edge detection and dominant height calculations (Rammer and Seidl 2015). At a broader level, stands are aggregated into 100 × 100 m Resource Units (RUs) for water balance and soil process calculations (Seidl et al. 2012).

This multi-scale spatial design ensured realistic ecological context for the central plot while preventing artificial isolation effects.

3.4 Tree Initialization

The initialization of individual trees in the Mathislewald study plot was based on a combination of terrestrial laser scanning (TLS) and a ground-truth field inventory, which together provided a high-resolution, spatially explicit dataset for iLand simulations. By integrating TLS-derived structural information with manually collected reference data, the approach ensured both geometric accuracy and ecological realism.

Ground-truth inventory

The ground-truth inventory recorded species, stem diameter, and tree position across the plot. Circumference at breast height was measured manually and converted to DBH. Tree heights were estimated from DBH using species-specific allometric functions from the R package *rBDAT* (Anerud et al., 2022). Species were identified visually by expert observers.

Tree positions were measured using an EMLID Reach 2+ RTK-GNSS system, with digital data entry via Open Data Kit (Hartung et al. 2010). GNSS measurements were taken 1 m north of each trunk to reduce canopy interference and corrected in post-processing. Coordinates were further refined in QGIS by aligning them with TLS-detected stem positions based on a 2 cm raster density map of the lower 2 m of the point cloud. Where ambiguity occurred, DBH served as a secondary matching criterion. This workflow produced a spatially consistent dataset used for both TLS validation and iLand initialization.

TLS data acquisition

TLS data were collected using a Riegl VZ-400i scanner at multiple positions to minimize occlusion. Scans were conducted with 0.04° angular resolution and 1200 kHz pulse repetition rate, from approximately 1.6 m above ground. Point clouds were preprocessed and co-registered in RiSCAN PRO (Larysch et al. 2025). Low-quality returns were removed, and data were downsampled to a uniform 2 cm voxel grid. The resulting 3D point cloud captured stem and crown structure with high accuracy, comparable to allometric and destructive measurements (Liang et al. 2016; Calders et al. 2020).

Tree segmentation and classification

TLS data were segmented and classified using deep learning approaches. The ForAINet model partitioned the point cloud into structural classes, achieving high detection accuracy (Xiang et al. 2024). Species classification was performed using the DetailView model (Frey and Schindler 2024b), trained on the FOR-species20K dataset (Puliti et al. 2025). Benchmarking indicates overall accuracies exceeding 0.8, particularly for dominant canopy species. For this study, DetailView was applied with weights optimized for Central European species (Frey and Schindler 2024b; Schindler and Frey 2024). Stem positions and DBH were derived using the *forest_inventory* function of the CSPStandSegmentation package (Frey and Schindler 2024a).

iLand initialization

Both GT and TLS inventories were exported as CSV files and applied to the central stand using single mode and single type initialization in iLand. This allowed parallel simulations under identical conditions.

Each record included Cartesian coordinates (x, y), species code, DBH, and total height, linked to the project's SQLite species database to ensure parameter consistency. Only the central plot contained explicit tree data; surrounding Forested Outside Pixels (FOPs) functioned as buffers providing competition and seed input (Section 3.3).

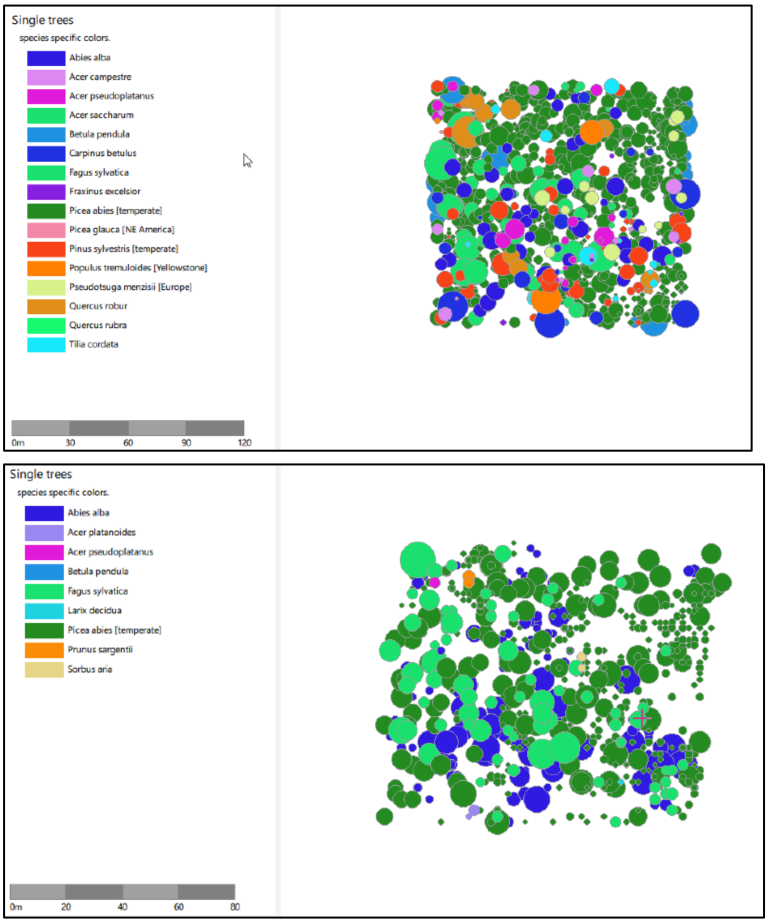

Figure 3 Initial tree initialization of the Mathislewald plot from RS based inventory (TLS), with size scaled to DBH.

3.5 Site Initialization (Soils, Snags, and Seed Dispersal)

In addition to the empirical tree initialization (Section 3.4), the iLand model requires several site-level inputs to represent edaphic conditions, legacy carbon pools, and regeneration dynamics. For this study, soil properties, snag pools, and seed dispersal were parameterized as follows.

Soil properties

Soil inputs were derived from regionalized datasets for Baden-Württemberg (Hartmann et al. 2024), combining data from the German National Soil Condition Survey (BZE II), the National Forest Inventory (BWI³), and additional geological profiles. These data were statistically regionalized using boosted regression tree (BRT) models stratified by natural regions, providing soil variables such as texture fractions, depth, bulk density, humus stock, and plant-available water capacity at 25 × 25 m resolution. For this study, soil depth and texture were selected as key variables influencing plant-available water in iLand. The 25 m rasters were resampled to the 100 m resource unit (RU) resolution to align with the simulation grid. While texture and depth were obtained from published maps (Hartmann 2024), nitrogen data were not publicly available. Provisional gridded nitrogen values were provided by Jonas Kerber (Technical University of Munich, pers. comm.) and should therefore be considered exploratory and more uncertain than the texture-based inputs.

Snag and soil carbon pools

Deadwood and soil organic matter pools were initialized using iLand's directed spin-up procedure rather than empirical measurements (Iland Documentation 2025). The model was run under baseline conditions until equilibrium of soil carbon and deadwood pools was reached, and the resulting state variables were exported as initialization snapshots for scenario runs. This approach avoids unrealistic zero baselines by incorporating a plausible legacy of past dynamics. Because these pools were not calibrated to site data, they are treated as model-based estimates, and analyses focus on scenario contrasts rather than absolute values.

Seed-belt configuration (seedDispersal)

Regeneration was simulated using the *seedDispersal* module in seedbelt mode, with a 10 m virtual belt divided into five site-type and two productivity classes (sizeX = 5, sizeY = 2). Each class was assigned species-specific regeneration probabilities representing relative establishment likelihoods following canopy openings. Probabilities were defined heuristically based on observed stand composition. *Picea abies* received the highest values (≈ 0.35–0.45), followed by *Fagus sylvatica* and *Abies alba* (≈ 0.20–0.30; 0.20–0.25), while *Acer pseudoplatanus* and *Pseudotsuga menziesii* were assigned lower probabilities (≈ 0.05–0.15). This configuration provides a continuous seed source consistent with the inventory and reduces edge effects, allowing climate-driven differences in seedling performance to shape competitive dynamics.

Species parameters and phenology

Species-specific parameters required by iLand (n = 66 per species) were taken from the curated iLand species database for 150 temperate and boreal species/provenances (Thom et al. 2024). We used the provided SQLite tables for *Picea abies*, *Fagus sylvatica*, and *Abies alba* and retained defaults unless stated otherwise. Parameter scope, definitions (e.g., fecundity_m2, seedKernel_as1/as2, snagKSW, snagHalfLife, snagKYR), and confidence categories are documented in the dataset's methods (Thom et al. 2024; Thom 2024).

3.6 Simulation Scenarios

The simulation experiment assessed forest growth and structural dynamics of the Mathislewald under RCP2.6, RCP4.5, and RCP8.5 for 2025–2100, representing low- to high-emission trajectories. For each scenario, a dedicated daily climate dataset (Section 3.2) was used, and simulations were initialized in 2025 from the observed 2024 forest state using both ground-truth (GT) and remote sensing (RS) inventories (Section 3.4). The <co2pathway> parameter was aligned with each RCP to ensure consistent CO_2 fertilization effects via the <CO2Response> module. Simulations operated at annual time steps, with light competition resolved at 2 m resolution (Seidl et al. 2012). Wind and bark beetle disturbances were disabled to isolate climate effects. Each scenario was replicated 100 times to account for stochasticity in mortality and regeneration. Replicates enabled estimation of mean trajectories and variability in basal area, stem density, biomass, and species composition. Outputs were stored separately for structured post-processing in R and Python.

3.7 Output Configuration and Analysis

All simulations were executed using the iLand console application, with outputs defined in the project configuration file. For each replicate, results were exported as SQLite databases, labeled by initialization type (RS or GT), climate scenario (RCP2.6, RCP4.5, RCP8.5), and replicate number to ensure traceability and automated post-processing. Only essential output tables were activated to minimize file size. Tree-level outputs recorded annual species identity, DBH, height, and biomass, from which increments, basal area, volume, and biomass accumulation were derived. Stand-level outputs summarized density, basal area, mean height, and leaf area index (LAI). Vertical structure was assessed using height-class distributions. Carbon cycling was evaluated through net primary production (NPP), respiration, and related fluxes, while mortality was quantified from annual biomass losses. Monthly gross primary productivity (GPP) was used to assess seasonal dynamics. All outputs were processed in R and Python using standard database, statistical, and visualization packages. For each replicate ($n = 100$ per scenario), variables were aggregated at stand level, and species-specific metrics were derived from tree records. Shannon diversity was calculated from species stem proportions. Climate scenario effects were tested using one-way ANOVA with Tukey's HSD post-hoc tests, and RS–GT differences at year 75 were assessed using Welch's t-tests. Statistical significance was defined at $p < 0.05$. Results were visualized using time-series ribbon plots, boxplots, stacked area charts for species composition, and seasonal GPP climatologies, highlighting mean trajectories and variability across replicates.

4. Results

This chapter presents simulation results for growth and productivity (4.1), species composition and diversity (4.2), structural development (4.3), mortality (4.4), and seasonal productivity (4.5).

Initial differences between remote sensing (RS) and ground-truth (GT) inventories explain early dynamics. RS included more stems, particularly suppressed individuals, resulting in higher initial density. GT contained fewer but larger trees, with higher mean DBH and height. Despite this, basal area was comparable due to larger GT diameters. RS simulations therefore began denser and showed stronger early self-thinning, while GT runs started with larger individuals. Species composition was similar, dominated by *Picea abies* and *Fagus sylvatica*, but RS included more minor species, leading to slightly higher initial richness. Overall, RS represented denser, smaller trees, whereas GT emphasized fewer, larger canopy trees, differences that shaped subsequent simulation trajectories.

4.1 Forest Growth and Productivity

Forest growth and productivity over the 75-year simulation differed strongly among climate scenarios (RCP2.6, RCP4.5, RCP8.5) and, to a lesser degree, between initialization datasets (RS vs. GT). Indicators included DBH and height increment, basal area, stem volume, biomass pools, and net primary productivity (NPP) at tree and stand levels. Results are first presented for RS simulations, followed by comparisons with GT to assess consistency and potential biases.

Growth increments (RS across scenarios)

Growth responses showed a clear dependence on climate forcing. With RS initialization, mean DBH increment at year 75 was highest under RCP4.5 (0.324 cm yr^{-1}), intermediate under RCP8.5 (0.268 cm yr^{-1}), and lowest under RCP2.6 (0.254 cm yr^{-1}). This ordering (RCP4.5 > RCP8.5 > RCP2.6) was consistent across replicate simulations and confirmed by Tukey post-hoc tests, which indicated that all pairwise differences were statistically significant ($p < 0.001$).

Table 1 Tukey HSD pairwise comparisons of mean DBH and Height increments (cm yr^{-1}) across climate scenarios (RCP2.6, RCP4.5, RCP8.5) at year 75, RS initialization

Variable	Adj. p-value
DBH increment	<0.001
DBH increment	<0.001
DBH increment	<0.001
Height increment	<0.001
Height increment	<0.001
Height increment	<0.001

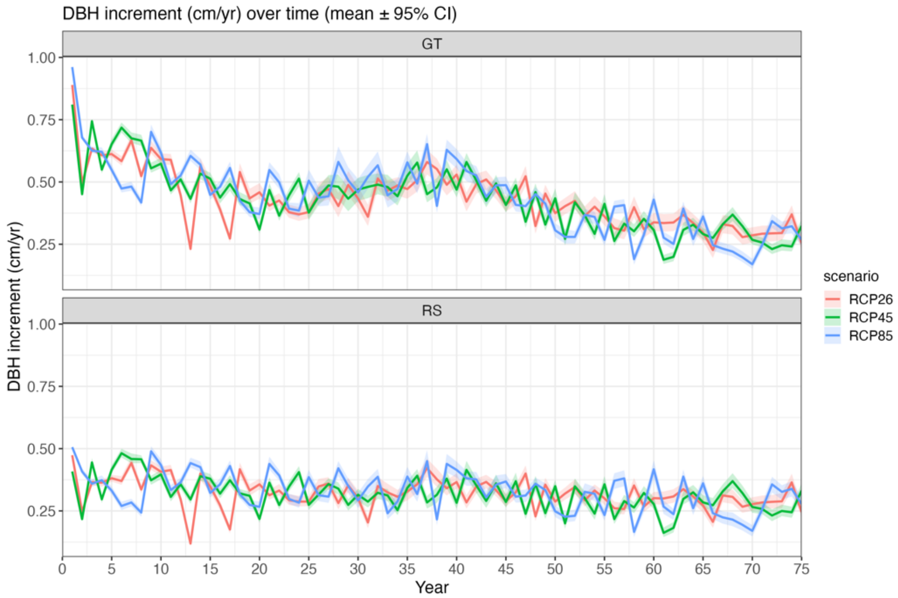

Figure 4 DBH increment trajectories (mean ± 95% CI) for RS and GT simulations under RCP2.6, RCP4.5, and RCP8.5 across 75 years.

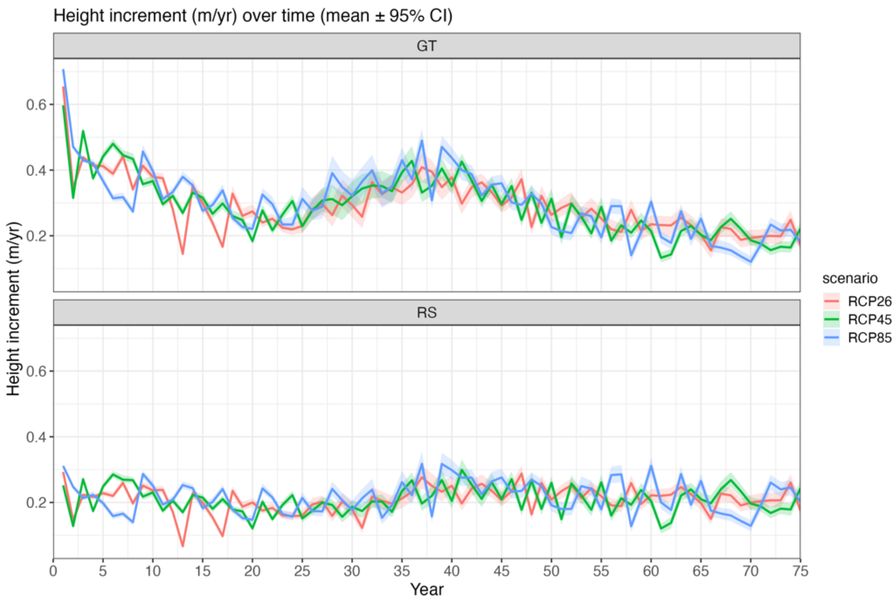

Figure 5 Height increment trajectories (mean ± 95% CI) for RS and GT across climate scenarios over 75 years.

Across RS simulations, DBH growth under RCP4.5 was 27.5% higher than RCP2.6, while RCP8.5 exceeded RCP2.6 by 5.5% but remained 17.2% below RCP4.5. Height increments followed the same pattern, reaching 0.223 cm yr^{-1} (RCP4.5), 0.182 cm yr^{-1} (RCP8.5), and 0.170 cm yr^{-1} (RCP2.6). Compared to RCP2.6, height growth increased by 30.6% under RCP4.5 and 6.9% under RCP8.5, but was 18.2% lower in RCP8.5 relative to RCP4.5. Over time, RCP4.5 maintained stable increments, whereas RCP8.5 declined in later decades, indicating intensifying stress. GT simulations showed the same scenario ranking but slightly higher absolute values. Mean DBH increments were 0.245 cm yr^{-1} (RCP2.6), 0.332 cm yr^{-1} (RCP4.5), and 0.278 cm yr^{-1} (RCP8.5), with height increments of 0.175, 0.228, and

0.203 cm yr^{-1}, respectively. Again, RCP4.5 sustained the strongest growth, while RCP8.5 declined toward the end of the simulation.

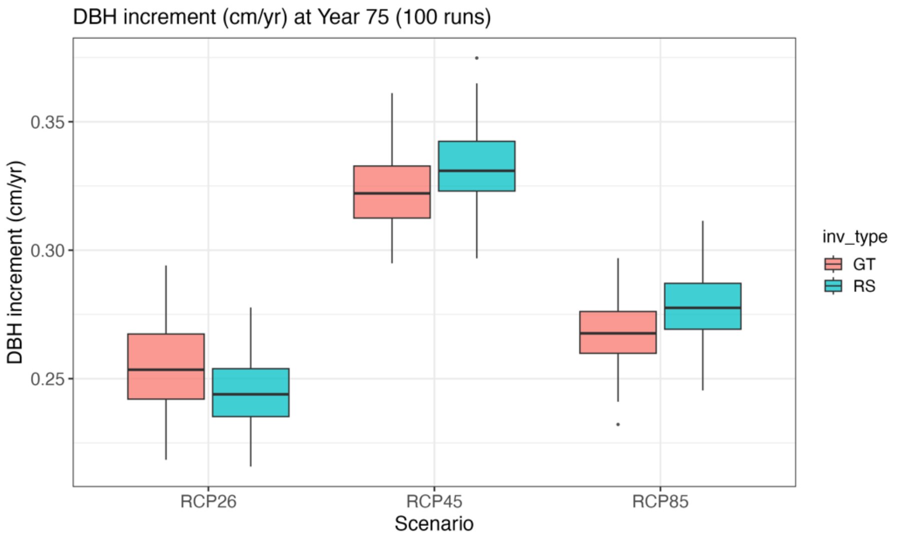

Figure 6 Boxplots of diameter increment at year 75 for RS and GT simulations across climate scenarios.

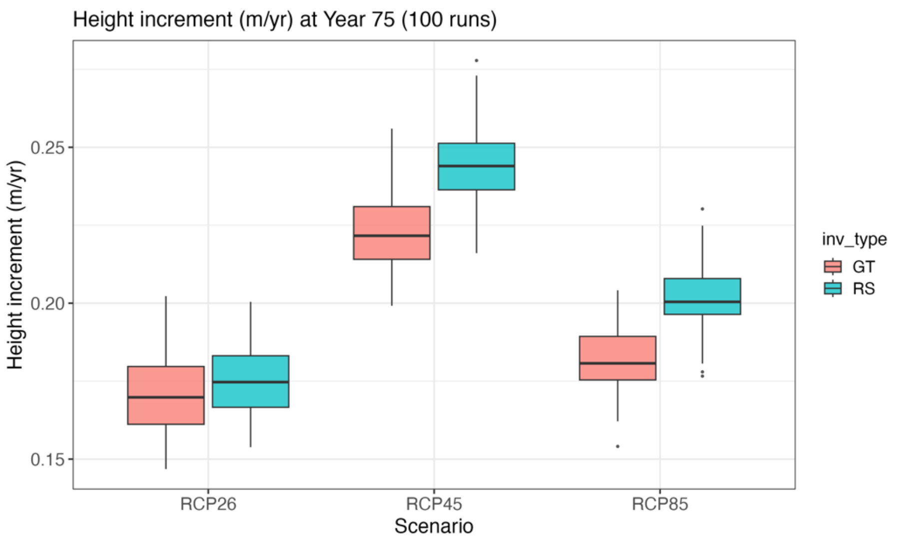

Figure 7 Boxplots of height increment at year 75 for RS and GT simulations across climate scenarios.

Net primary productivity

Net primary productivity (NPP) exhibited the strongest and most consistent scenario signal. At year 75, RS-initialized NPP was highest in RCP4.5 (10,999 g C m^{-2} yr^{-1}), followed closely by RCP8.5 (10,742 g C m^{-2} yr^{-1}), with RCP2.6 lowest (9,576 g C m^{-2} yr^{-1}). This translates to a +1,423 g C m^{-2} yr^{-1} increase (+14.9%) from RCP2.6 to RCP4.5, and a +1,166 g C m^{-2} yr^{-1} increase (+12.2%) from RCP2.6 to RCP8.5, while RCP8.5 remained 2.3% below RCP4.5. All pairwise contrasts were significant ($p < 0.001$).

Table 2 Tukey HSD post-hoc comparisons for net primary productivity (NPP, g C m⁻² yr⁻¹) at year 75 between climate scenarios (RS initialization)

Scenario Contrast	Mean Diff (g C m^{-2} yr^{-1})	95% CI Low	95% CI High	Adj. p-value
RCP4.5 – RCP2.6	1423.079	1387.039	1459.120	<0.001
RCP8.5 – RCP2.6	1166.365	1130.324	1202.405	<0.001
RCP8.5 – RCP4.5	–256.715	–292.755	–220.674	<0.001

Temporal dynamics under RS simulations show that RCP4.5 maintained elevated productivity throughout the simulation, whereas RCP8.5 initially approached RCP4.5 levels but began to decline towards the end of the period, likely reflecting increasing heat and water limitations. This non-linear response suggests that moderate warming and elevated CO_2 can enhance productivity, but the benefits diminish under stronger climate forcing.

The GT simulations showed broadly similar trajectories, with higher absolute values across scenarios. By year 75, mean NPP reached 9,815 g C m^{-2} yr^{-1} in RCP2.6, 11,274 g C m^{-2} yr^{-1} in RCP4.5, and 11,056 g C m^{-2} yr^{-1} in RCP8.5. The overall pattern was consistent with RS, with strongest productivity under RCP4.5, slightly lower under RCP8.5, and lowest under RCP2.6.

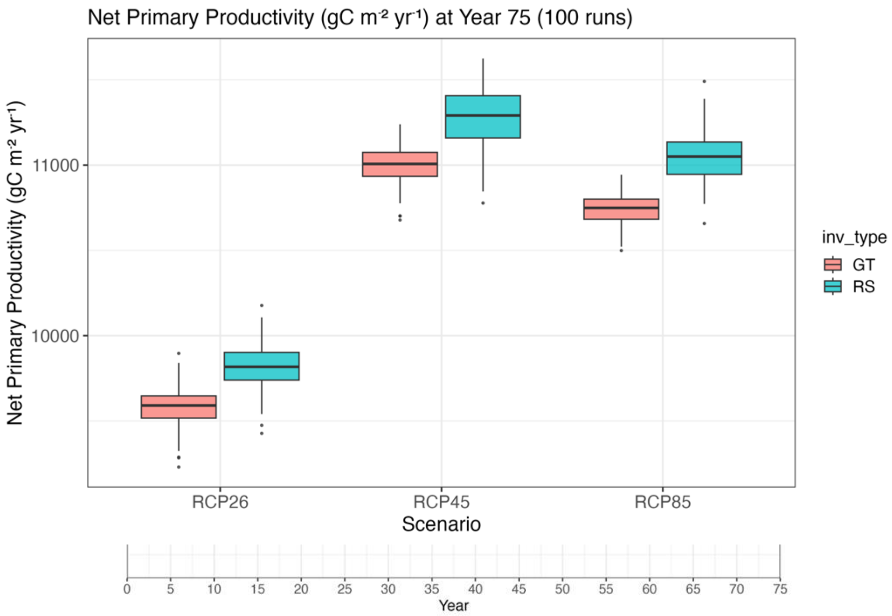

Figure 8 Boxplots of NPP at year 75 across RCP scenarios for RS and GT simulations.

Structural stocks and biomass (RS across scenarios)

Across RS runs, while increments and NPP peaked under RCP4.5, structural stocks such as basal area, volume, and biomass reached their highest values under RCP8.5. Basal area at year 75 averaged 82.96 m^2 ha^{-1} in RCP8.5, compared to 79.99 in RCP4.5 and 78.86 in RCP2.6. The GT simulations produced higher absolute values but exhibited the same scenario ordering. By year 75, basal area reached 104.5 m^2 ha^{-1} in RCP2.6, 106.9 m^2 ha^{-1} in RCP4.5, and 110.2 m^2 ha^{-1} in RCP8.5.

The GT simulations produced higher absolute values but exhibited the same scenario ordering. By year 75, basal area reached 104.5 m^2 ha^{-1} in RCP2.6, 106.9 m^2 ha^{-1} in RCP4.5, and 110.2 m^2 ha^{-1} in RCP8.5.

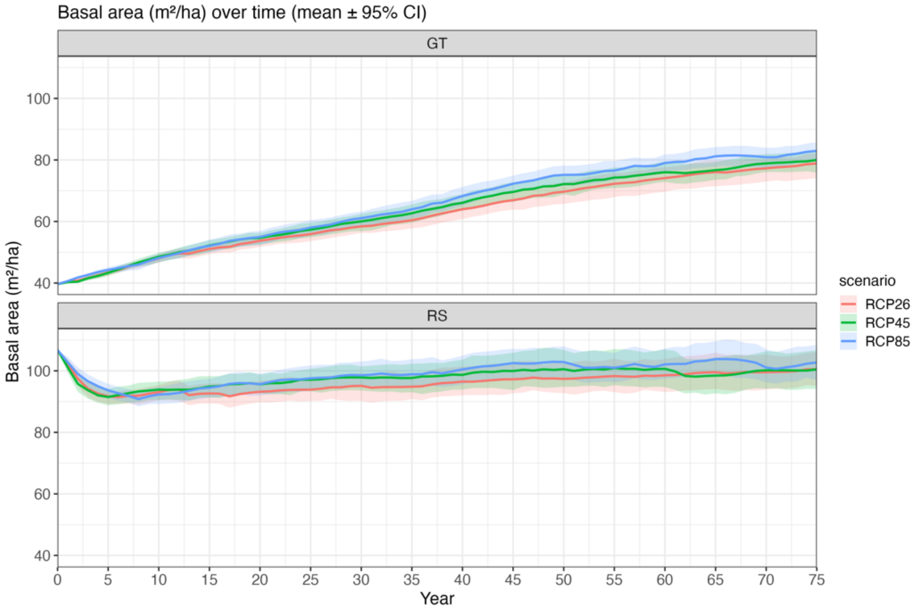

Figure 9 Basal area trajectories (mean ± 95% CI) for RS and GT simulations across 75 years under climate scenarios.

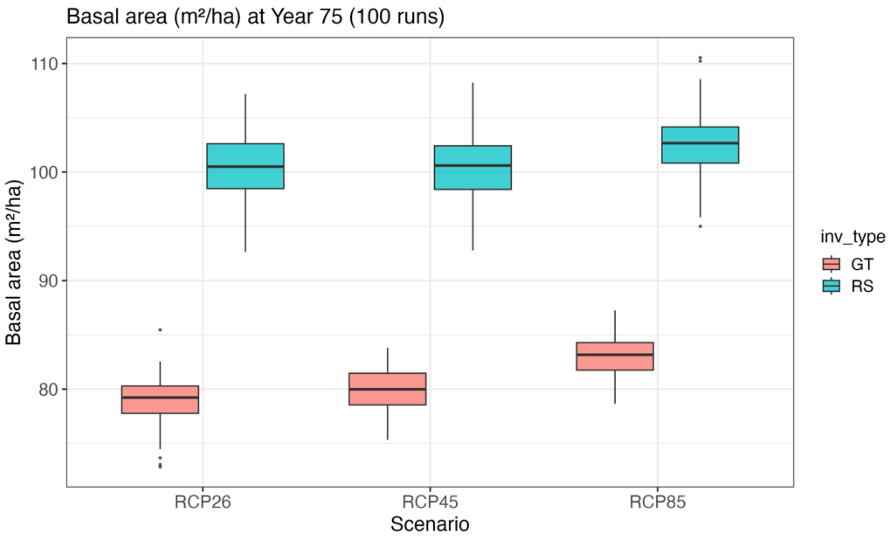

Figure 10 Boxplots of basal area at year 75 for RS and GT simulations across scenarios.

Under RS simulations, stem volume followed the same pattern, with means of 1,091.8 $m^3 ha^{-1}$ in RCP8.5, 1,048.3 $m^3 ha^{-1}$ in RCP4.5, and 1,033.7 $m^3 ha^{-1}$ in RCP2.6. Stem volume values were 1,170.2 $m^3 ha^{-1}$ in RCP2.6, 1,201.4 $m^3 ha^{-1}$ in RCP4.5, and 1,247.8 $m^3 ha^{-1}$ in RCP8.5 of GT simulations.

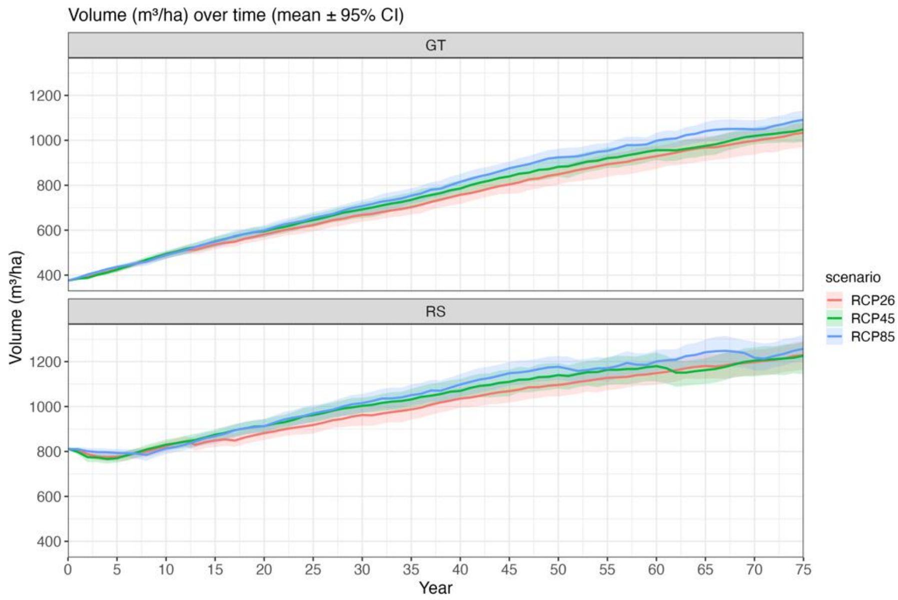

Figure 11 Stem volume trajectories (mean ± 95% CI) for RS and GT simulations under three RCP scenarios across 75 years.

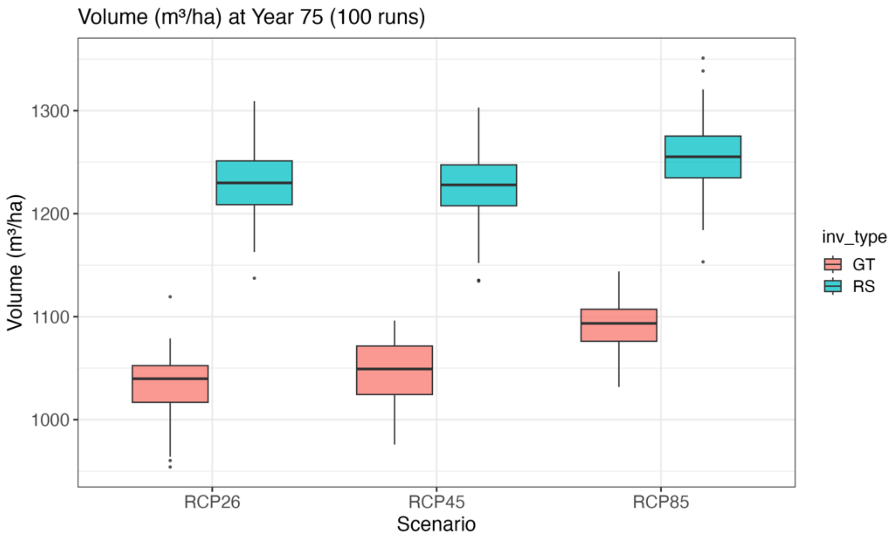

Figure 12 Boxplots of stem volume at year 75 across RCP scenarios for RS and GT simulations.

Similarly, across RS simulations, total biomass accumulated to 771.7 Mg ha^{-1} under RCP8.5, compared to 740.3 Mg ha^{-1} (RCP4.5) and 728.3 Mg ha^{-1} (RCP2.6). Tukey tests confirmed that RCP8.5 was significantly greater than both RCP2.6 and RCP4.5, while differences between RCP4.5 and RCP2.6 were small and often not significant. Under GT runs, total biomass accumulated to 935.6 Mg ha^{-1} in RCP2.6, 960.2 Mg ha^{-1} in RCP4.5, and 988.7 Mg ha^{-1} in RCP8.5.

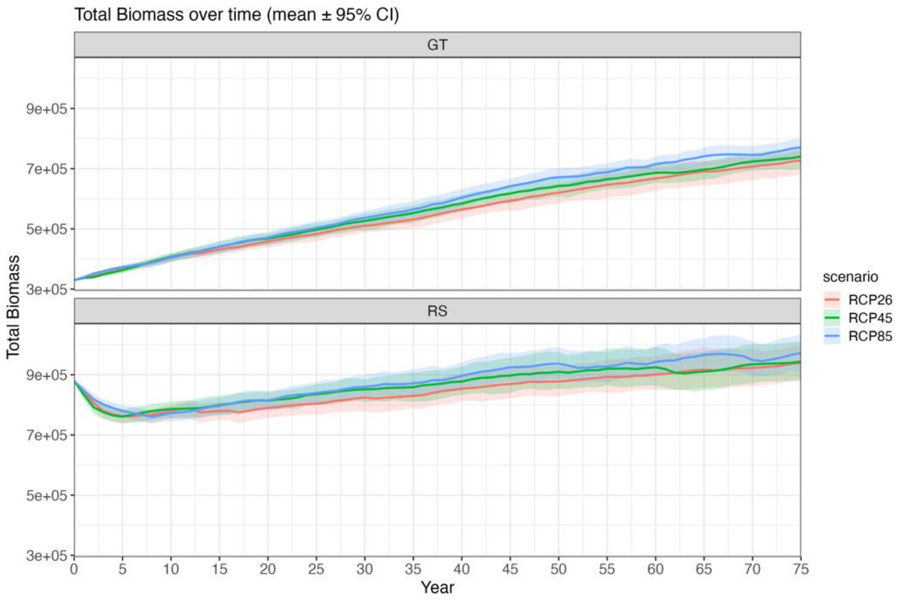

Figure 13 Total biomass accumulation trajectories (mean ± 95% CI) for RS and GT across climate scenarios over 75 years.

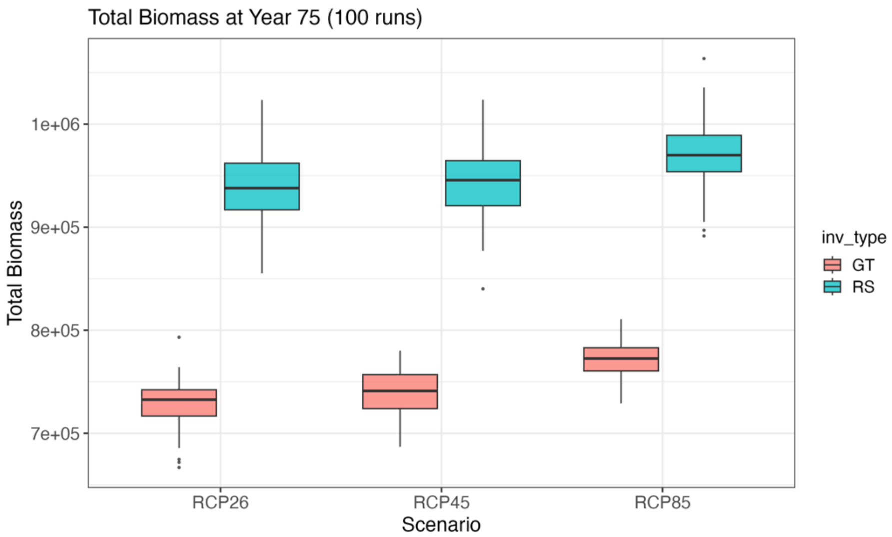

Figure 14 Boxplots of total biomass at year 75 for RS and GT simulations across scenarios.

These results indicate that, although growth rates slowed under the harsher scenario, cumulative biomass accumulation over 75 years was still greatest under RCP8.5, likely because mortality reductions and CO_2 fertilization effects partly offset stressinduced declines in increments.

Table 3 Tukey HSD results for Basal area, Volume, and Total biomass at year 75 (RS simulations).

Variable	Scenario Contrast	Mean Diff	95% CI Low	95% CI High	Adj. p-value
Basal area (m^2 ha^{-1})	RCP45–RCP26	–0.031	–1.034	0.972	0.997
Basal area (m^2 ha^{-1})	RCP85–RCP26	2.189	1.186	3.193	<0.001

Variable	Scenario Contrast	Mean Diff	95% CI Low	95% CI High	Adj. p-value
Basal area (m² ha⁻¹)	RCP85–RCP45	2.220	1.217	3.224	<0.001
Volume (m³ ha⁻¹)	RCP45–RCP26	–2.815	–13.980	8.350	0.823
Volume (m³ ha⁻¹)	RCP85–RCP26	27.844	16.679	39.009	<0.001
Volume (m³ ha⁻¹)	RCP85–RCP45	30.659	19.494	41.824	<0.001
Total biomass (Mg ha⁻¹)	RCP45–RCP26	5185.900	–5816.170	16188.000	0.508
Total biomass (Mg ha⁻¹)	RCP85–RCP26	33059.900	22057.800	44062.000	<0.001
Total biomass (Mg ha⁻¹)	RCP85–RCP45	27874.000	16871.900	38876.100	<0.001

4.2 Species Composition and Diversity

Species composition and diversity indicate how forests reorganize under climate change. This section focuses primarily on the remote sensing (RS) initialization, with ground-truth (GT) results presented for comparison. Analysis includes (i) temporal species trajectories, (ii) end-of-simulation dominance (year 75), and (iii) Shannon diversity dynamics.

Temporal Dynamics of Species Composition

At initialization, the RS dataset was dominated by *Picea abies*, contributing over half of stems and basal area. Although spruce remained dominant throughout the 75-year simulations, its share declined with increasing climate forcing.

Under RCP2.6, spruce still accounted for over 80% of basal area, with gradual gains by *Fagus sylvatica* and *Abies alba*. In RCP4.5, spruce declined to ~79%, while beech (10.5%) and fir (5.9%) expanded. Under RCP8.5, spruce further decreased to 76.5%, with beech rising to 11.8% and fir stabilizing at ~5.7%. Minor species showed small but consistent increases, indicating progressive diversification under stronger warming. GT simulations showed the same trend but with higher spruce persistence (82.5%, 81.2%, and 79.4% under RCP2.6, 4.5, and 8.5). Accordingly, beech and fir expanded less strongly, and minor species gains were marginal.

Overall, both datasets indicate declining spruce dominance under warming, but RS projects faster compositional shifts toward mixed stands, whereas GT suggests greater spruce stability.

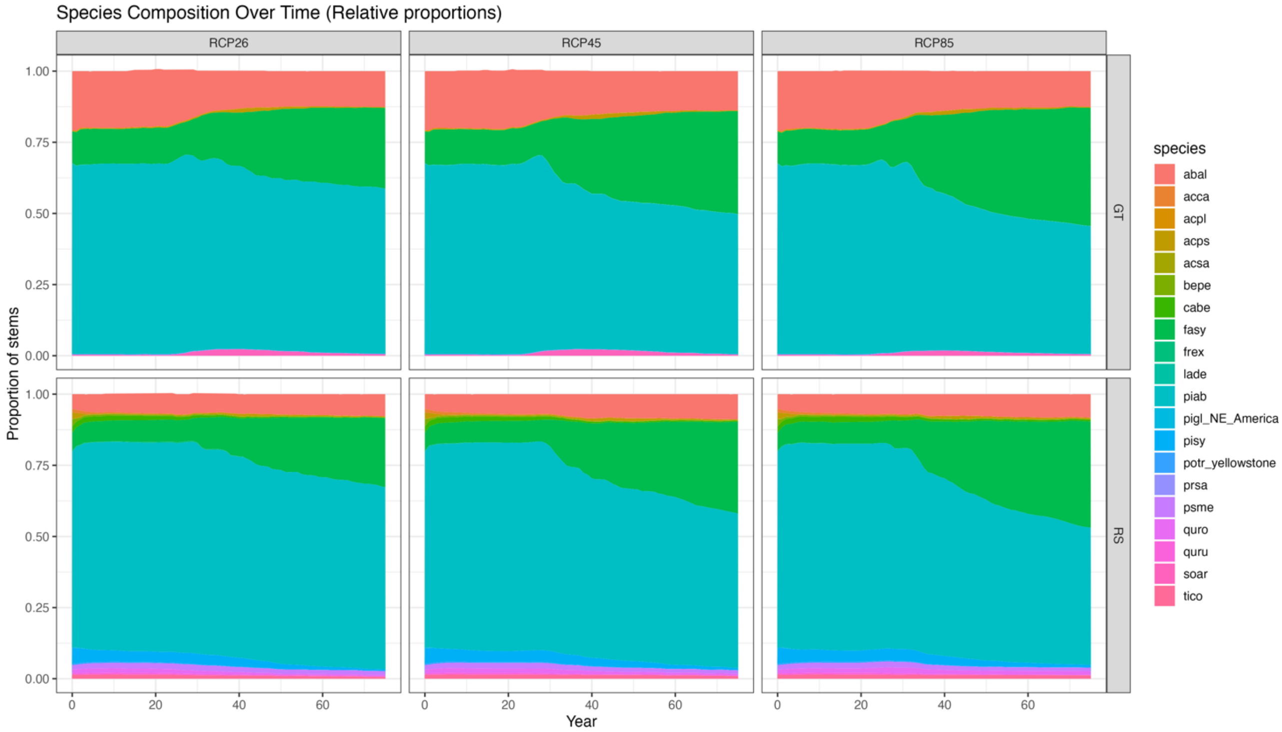

Figure 16 Temporal development of species composition expressed as absolute stem counts over 75 years under three climate scenarios (RCP2.6, RCP4.5, and RCP8.5). Results are shown separately for the ground truth (GT, upper panels) and remote sensing (RS, lower panels) inventories.

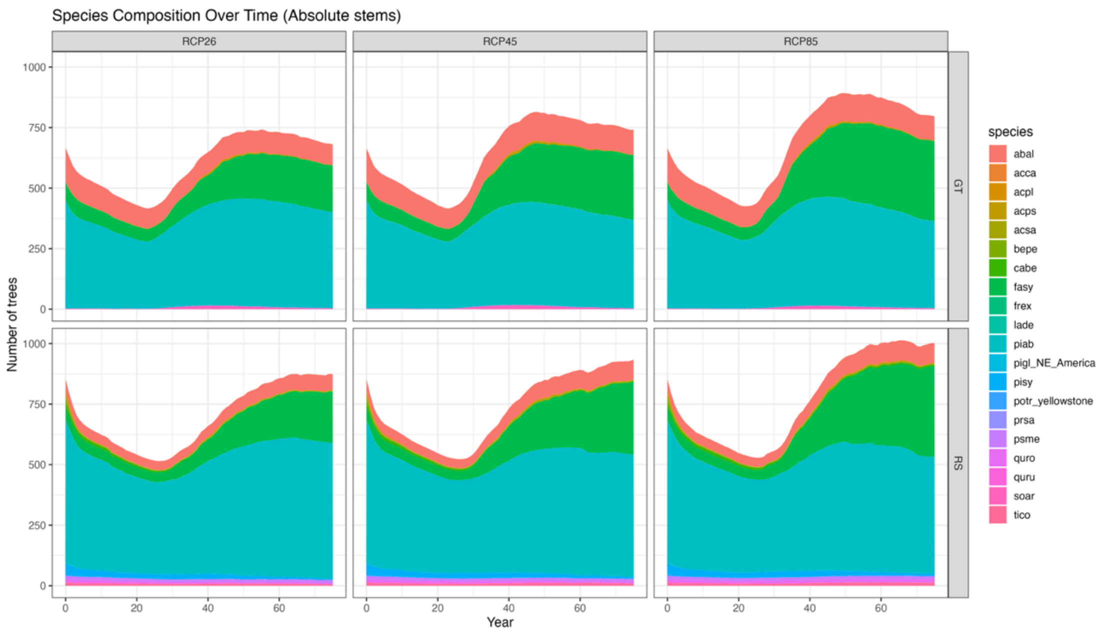

Figure 15 Temporal development of species composition expressed as relative proportions of stems over 75 years under three climate scenarios (RCP2.6, RCP4.5, and RCP8.5). Results are shown separately for the GT (upper panels) and RS (lower panels) inventories.

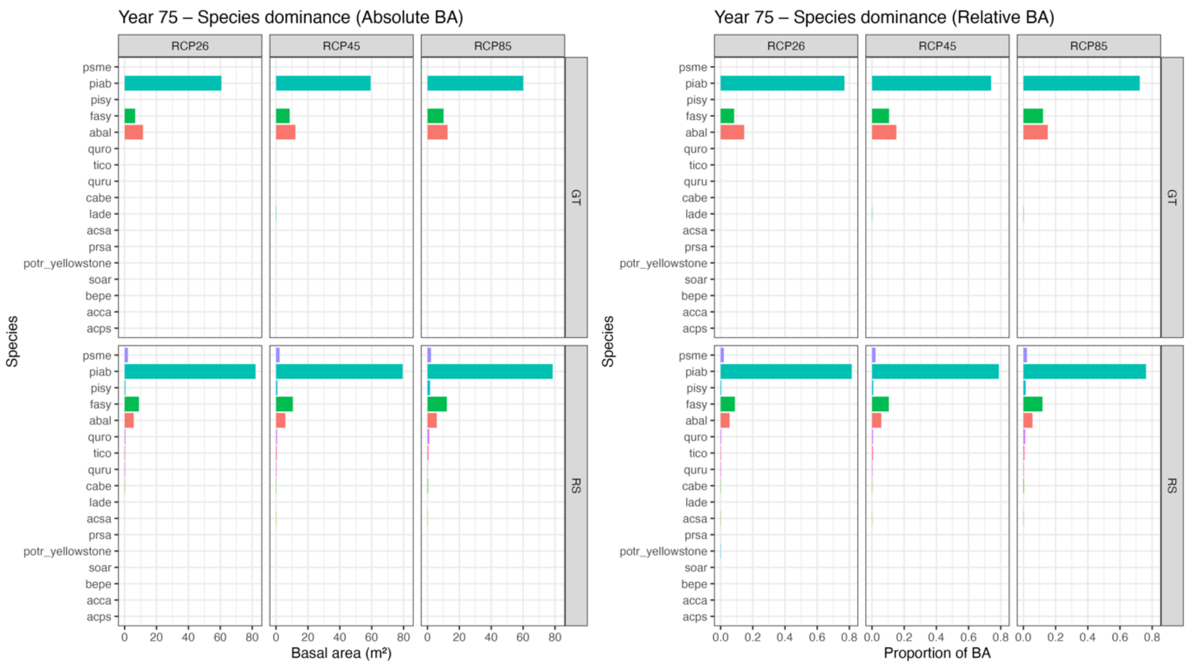

Figure 17 Species dominance at year 75 expressed as basal area. Left panels show absolute basal area (m² ha⁻¹), and right panels show relative basal area (proportion of stand total). Results are presented for GT (upper panels) and RS (lower panels) inventories across the three climate scenarios.

End-State Species Dominance

By year 75, RS simulations showed clear scenario-dependent shifts. Under RCP2.6, *Picea abies* remained dominant (81.4% basal area), with *Fagus sylvatica* (8.9%) and *Abies alba* (5.7%) secondary, and minor roles for *Pinus sylvestris* (0.5%) and *Acer pseudoplatanus*.

In RCP4.5, spruce declined to 78.8%, while beech increased to 10.5% and fir remained stable (~5.8%). Under RCP8.5, spruce further decreased to 76.2%, beech rose to 11.8%, and pine doubled to 1.5%, indicating gradual diversification under stronger warming. GT simulations projected lower spruce dominance but stronger fir persistence. Spruce accounted for 76.9%, 74.0%, and 72.4% under RCP2.6, 4.5, and 8.5, respectively, while fir consistently reached ~15%. Beech increased moderately (8.4–12.2%), and pine and maple remained negligible. Overall, RS projected a spruce-dominated but gradually diversifying canopy, whereas GT emphasized fir as a persistent co-dominant species. These differences highlight how initial inventory structure shapes long-term dominance patterns.

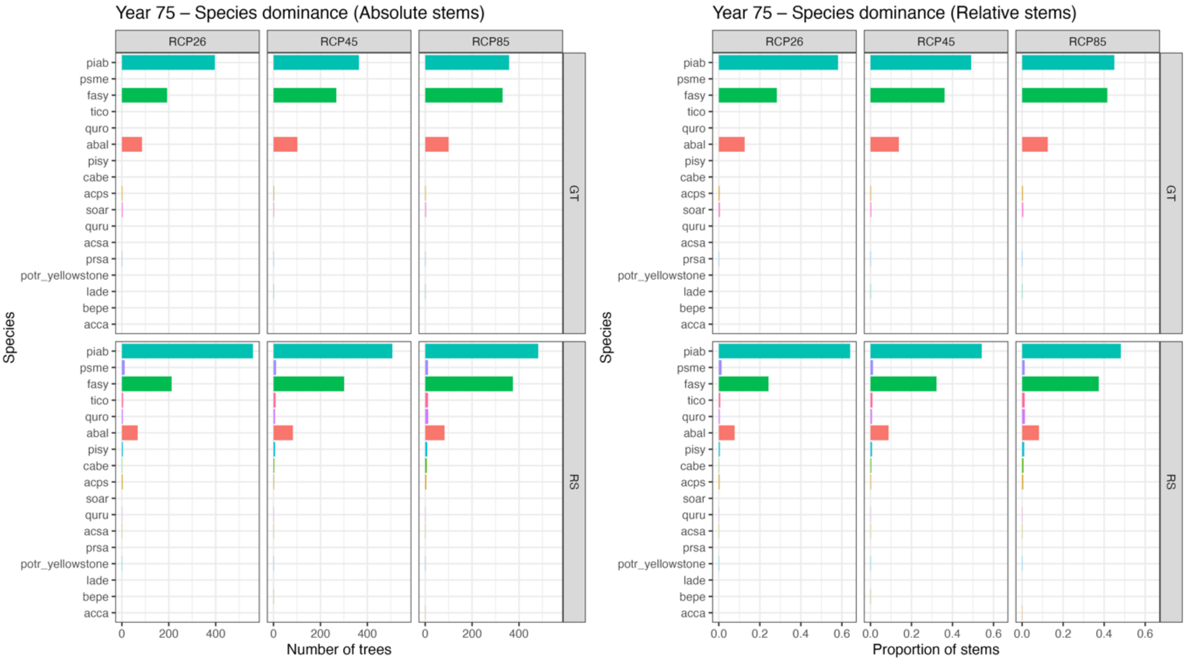

Figure 18 Species dominance at year 75 expressed as stem numbers. Left panels show absolute numbers of stems, and right panels show relative proportions of stems. Results are presented for GT (upper panels) and RS (lower panels) inventories across the three climate scenarios.

Diversity Dynamics

Shannon diversity mirrored scenario-dependent dominance shifts (Figure 21). In RS simulations, mean values at year 75 increased from 0.994 (RCP2.6) to 1.110 (RCP4.5) and 1.190 (RCP8.5), indicating progressive diversification with warming. The moderate rise under RCP4.5 reflected greater balance among spruce, beech, and fir, while RCP8.5 showed nearly 20% higher diversity than RCP2.6 due to reduced spruce dominance and contributions from minor species.

GT simulations showed the same trend but lower values: ~0.95 (RCP2.6), 1.04 (RCP4.5), and 1.10 (RCP8.5). RS consistently projected higher evenness, especially under RCP8.5, owing to weaker spruce persistence and stronger establishment of minor species compared to GT.

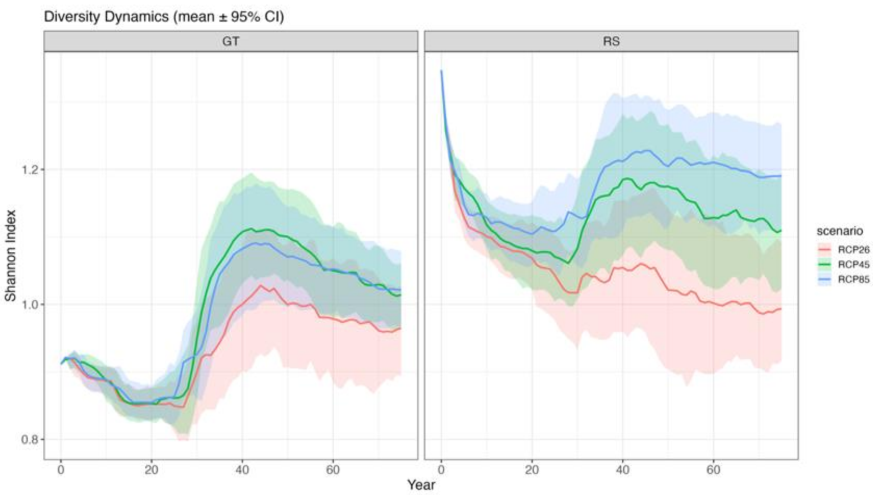

Figure 19 Shannon diversity index (mean ± 95% confidence intervals) over 75 years under three climate scenarios (RCP2.6, RCP4.5, and RCP8.5), for GT (left panel) and RS (right panel) simulations.

Statistical Comparisons of Dominant Species

Pairwise t-tests of basal area at year 75 provided statistical confirmation of these compositional shifts. In the RS simulations, beech increased significantly across all contrasts (RCP4.5 > RCP2.6, RCP8.5 > RCP2.6, and RCP8.5 > RCP4.5), while spruce exhibited significant declines with warming, particularly between RCP2.6 and the higher-forcing scenarios. Pine and maple also showed significant gains under RCP8.5, despite their relatively small overall shares.

The GT simulations highlighted a different set of transitions. Fir exhibited highly significant gains across all scenario contrasts, while beech also increased consistently with warming. Spruce declined significantly between RCP2.6 and RCP4.5, though its loss was less marked than in RS. *Sorbus aucuparia* emerged as a minor but statistically significant beneficiary under RCP8.5.

Table 4 Pairwise t-tests of species basal area at year 75. Only significant differences ($p < 0.05$) are shown. " > " indicates which scenario had higher basal area.

Species	Inventory	RCP4.5 vs RCP2.6	RCP8.5 vs RCP2.6	RCP8.5 vs RCP4.5
Picea abies (Norway spruce)	RS	RCP2.6 > RCP4.5 ($p = 1.5 \times 10^{-8}$)	RCP2.6 > RCP8.5 ($p = 6.8 \times 10^{-13}$)	n.s.
	GT	RCP2.6 > RCP4.5 ($p = 1.8 \times 10^{-5}$)	n.s.	RCP8.5 > RCP4.5 ($p = 9.7 \times 10^{-3}$)
Fagus sylvatica (European beech)	RS	RCP4.5 > RCP2.6 ($p = 9.8 \times 10^{-10}$)	RCP8.5 > RCP2.6 ($p = 9.0 \times 10^{-30}$)	RCP8.5 > RCP4.5 ($p = 6.6 \times 10^{-10}$)
	GT	RCP4.5 > RCP2.6 ($p = 9.9 \times 10^{-39}$)	RCP8.5 > RCP2.6 ($p = 1.5 \times 10^{-86}$)	RCP8.5 > RCP4.5 ($p = 5.4 \times 10^{-32}$)
Abies alba (Silver fir)	RS	n.s.	n.s.	n.s.
	GT	RCP4.5 > RCP2.6 ($p = 1.35 \times 10^{-3}$)	RCP8.5 > RCP2.6 ($p = 2.3 \times 10^{-8}$)	RCP8.5 > RCP4.5 ($p = 1.3 \times 10^{-2}$)
Pinus sylvestris (Scots pine)	RS	RCP4.5 > RCP2.6 ($p = 1.2 \times 10^{-4}$)	RCP8.5 > RCP2.6 ($p = 1.3 \times 10^{-26}$)	RCP8.5 > RCP4.5 ($p = 4.7 \times 10^{-14}$)
	GT	n.s.	n.s.	n.s.
Acer saccharum (Sugar maple)	RS	n.s.	RCP8.5 > RCP2.6 ($p = 2.4 \times 10^{-2}$)	n.s.
	GT	n.s.	n.s.	n.s.
Acer pseudoplatanus (Sycamore maple)	RS	n.s.	RCP8.5 > RCP2.6 ($p = 6.6 \times 10^{-5}$)	RCP8.5 > RCP4.5 ($p = 5.6 \times 10^{-7}$)
	GT	RCP8.5 > RCP2.6 ($p = 2.99 \times 10^{-2}$)	n.s.	n.s.
Sorbus aucuparia (Rowan)	RS	n.s.	n.s.	n.s.
	GT	RCP8.5 > RCP2.6 ($p = 3.3 \times 10^{-5}$)	RCP8.5 > RCP4.5 ($p = 8.7 \times 10^{-6}$)	n.s.

Overall, climate forcing drives a gradual reorganization of species composition in Mathislewald. RS simulations show declining spruce dominance with warming, alongside gains by beech, fir, and minor species, resulting in higher diversity under RCP8.5. GT simulations confirm the same trend but indicate slower transitions and stronger persistence of spruce and fir. These results demonstrate that climate change promotes diversification and reduces spruce dominance, while also highlighting the influence of initialization data: RS projects faster structural change, whereas GT suggests a more conservative trajectory over the 75-year horizon.

4.3 Structural Development

Structural attributes of the Mathislewald stands were evaluated through stem density, mean tree height, leaf area index (LAI), and vertical layering derived from dynamic stand height-class distributions. These indicators capture both horizontal (density, LAI) and vertical (height, canopy layering) aspects of stand development. Results are reported for the remote sensing (RS) initialization, followed by the ground truth (GT) initialization for comparison, and a statistical synthesis of RS and GT differences.

Tree Density

In the RS initialization, stand density increased consistently with climate forcing (Fig. 22, Fig. 23). At year 75, average stem numbers reached 515 ± 12 ha^{-1} under RCP2.6, 550 ± 15 ha^{-1} under RCP4.5, and 590 ± 18 ha^{-1} under RCP8.5 (mean ± SD across 100 replicates). Analysis of variance confirmed highly significant differences among scenarios ($F = 179.5$, $p < 0.001$; Table 6). The trajectory indicates that warmer conditions promoted denser stands, reflecting enhanced regeneration and survival under elevated temperatures.

In the GT simulations, densities also rose with increasing forcing but absolute values remained markedly lower. Final densities ranged between ~310 and 350 stems ha^{-1}, depending on scenario, confirming the tendency toward more open forests when initialized with ground-based inventory data.

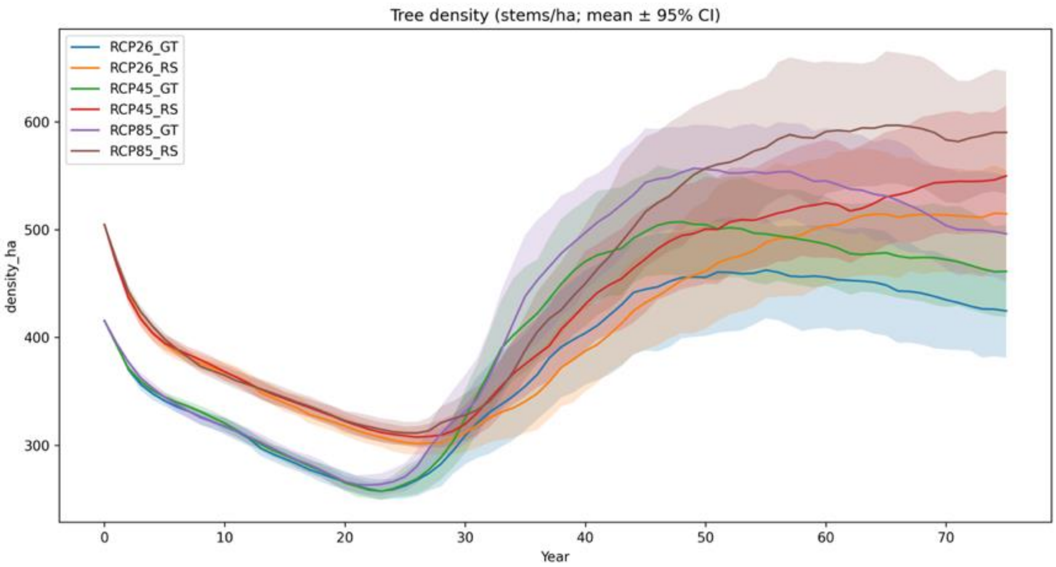

Figure 20 Tree density trajectories (mean ± 95% CI) for RS and GT simulations across climate scenarios over 75 years .

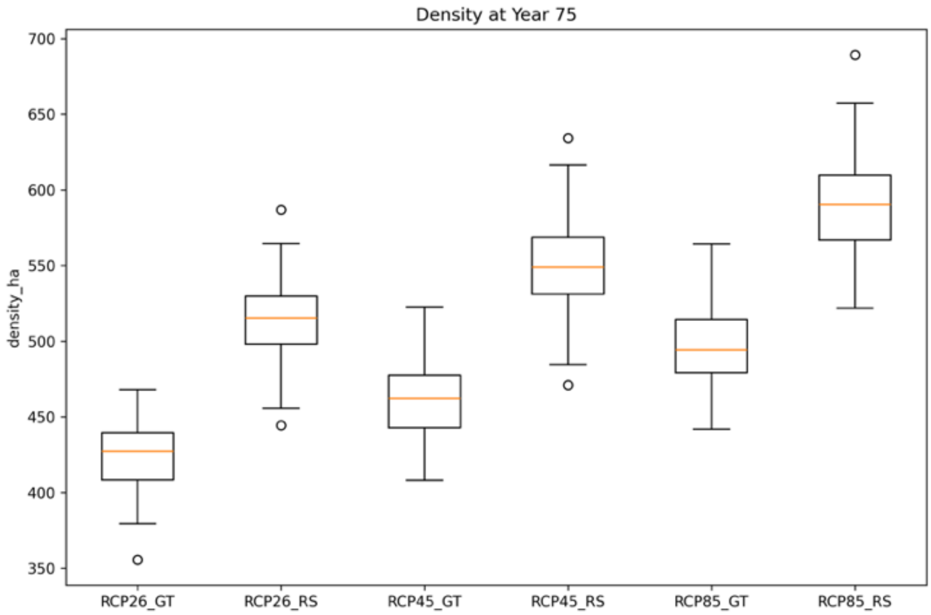

Figure 21 Boxplots of tree density at year 75 under RCP2.6, RCP4.5, and RCP8.5 for RS and GT simulations.

Table 5 ANOVA results for structural attributes (RS initialization only) across climate scenarios.

Variable	Year	RCP2.6 mean	RCP4.5 mean	RCP8.5 mean	F-statistic	p-value
Height (m)	75	17.923	17.144	16.944	114.219	<0.001
Density (stems ha^{-1})	75	514.805	549.964	590.343	179.514	<0.001
LAI	70	0.913	0.838	0.843	26.717	<0.001

Mean Tree Height

Height trajectories revealed an inverse response to density. In RS simulations, mean canopy height declined systematically with warming (Fig. 24, Fig. 25). Final heights averaged 17.9 ± 0.2 m under RCP2.6, 17.1 ± 0.2 m under RCP4.5, and 16.9 ± 0.3 m under RCP8.5. ANOVA results confirmed strong scenario effects ($F = 114.2$, $p < 0.001$; Table 6). These results demonstrate that increased density was accompanied by constraints on vertical growth, as competition limited tree height development (see Table 6). GT runs consistently produced taller forests, with end-state heights between 19 and 20 m across scenarios. Although warming also reduced canopy height, the effect was weaker than in RS, indicating that reduced crowding facilitated greater vertical development.

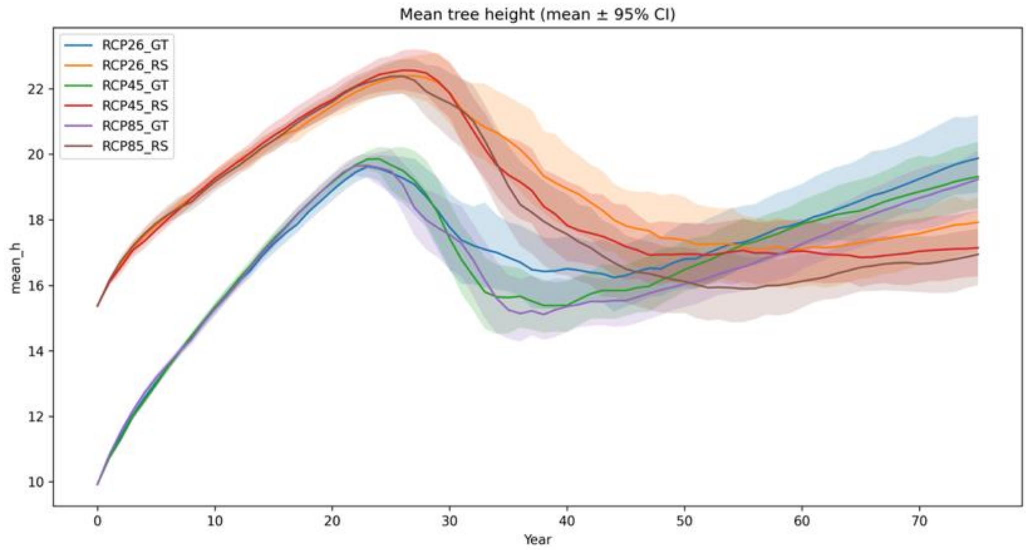

Figure 22 Mean tree height trajectories (mean ± 95% CI) for RS and GT simulations across scenarios over 75 years.

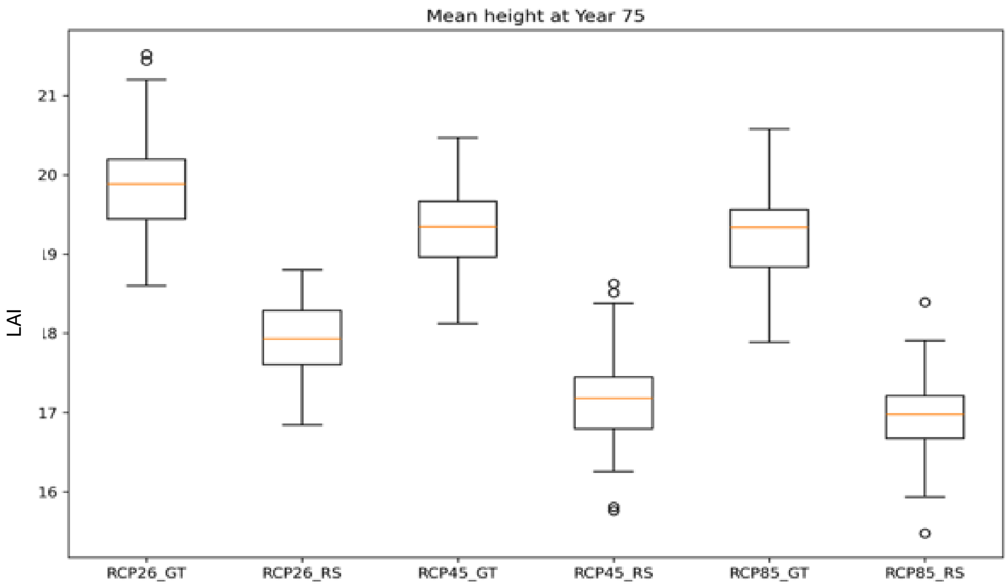

Figure 23 Boxplots of mean tree height at year 75 for RS and GT simulations.

Leaf Area Index (LAI)

LAI exhibited a modest but consistent decline with increasing climate forcing in RS simulations (Fig. 22, Fig. 23). By year 70, average values were 0.91 ± 0.02 under RCP2.6, 0.87 ± 0.02 under RCP4.5, and 0.84 ± 0.03 under RCP8.5. Scenario effects were significant ($F = 26.7$, $p < 0.001$; Table 6). The results indicate that despite higher stem densities, leaf area per unit ground area decreased under warmer scenarios, pointing to smaller average crown sizes and reduced foliage biomass.

GT results produced slightly higher LAI values (~1.0 on average at year 70) and weaker scenario contrasts. This reflects the presence of fewer but larger individuals in GT, sustaining comparable leaf area despite lower densities.

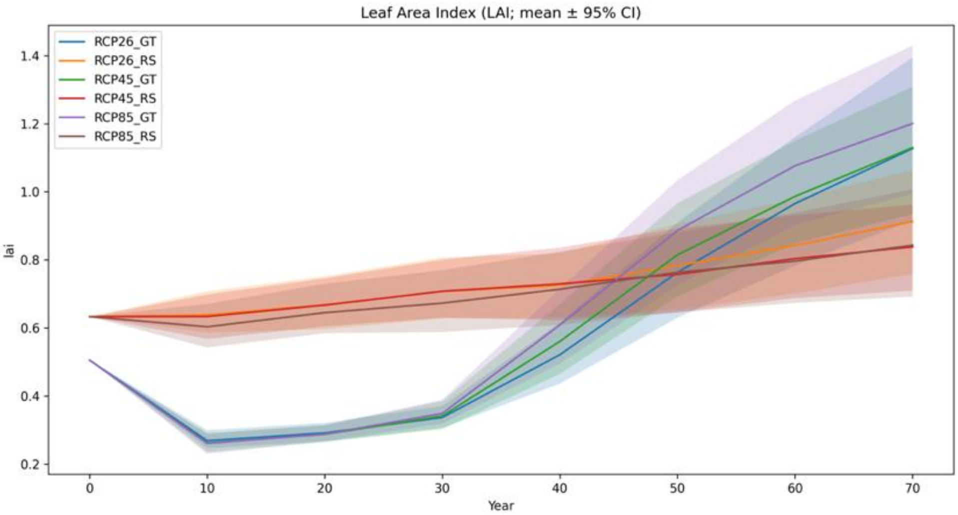

Figure 24 Leaf Area Index (LAI) trajectories (mean ± 95% CI) under RS and GT simulations across climate scenarios, up to year 70.

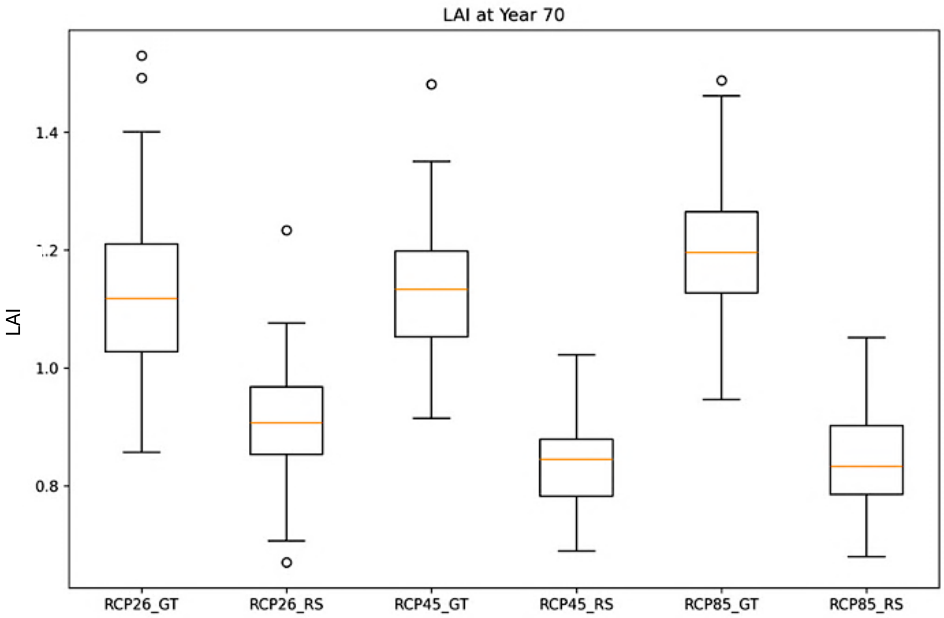

Figure 25 Boxplots of LAI at year 70 for RS and GT simulations across RCP scenarios.

4.4 Mortality and Disturbance Proxies

´Stand-level mortality was derived from iLand's *treeremoved* table as total annual biomass loss (kg yr^{-1}), summing stem, branch, foliage, and root components. As wind, bark beetle, and management were disabled, removals reflect intrinsic processes such as self-thinning and climate stress. For each scenario and inventory (RS, GT), 100 runs were analyzed. Results are presented as mean ± SD, with Welch's t-tests applied to cumulative mortality (Mg) across runs.

Annual and cumulative mortality

Annual removals showed an initial adjustment phase followed by stabilization. During years 1–3, RS removals averaged approximately 48 Mg yr^{-1} (47.1 Mg in RCP2.6 and 48.1 Mg in RCP4.5, with RCP8.5 of comparable magnitude). From year 4 onward, values stabilized near 10 Mg yr^{-1}, with a consistent climate ordering of 9.29 Mg yr^{-1} under RCP2.6, 9.47 Mg yr^{-1} under RCP4.5, and 10.06 Mg yr^{-1} under RCP8.5. This temporary increase at the beginning of the simulation did not alter the long-term ranking, which remained highest in RCP8.5, intermediate in RCP4.5, and lowest in RCP2.6. Run-level cumulative losses (mean ± SD, Mg) increased progressively with scenario severity, amounting to 809.1 ± 38.2 in RCP2.6, 825.8 ± 35.3 in RCP4.5, and 852.3 ± 34.2 in RCP8.5. Relative to RCP2.6, cumulative losses were 2.1% higher in RCP4.5 and 5.3% higher in RCP8.5, with RCP8.5 also exceeding RCP4.5 by 3.2%.

GT exhibits the same qualitative behavior at lower magnitude. The early adjustment is modest (≈ 5 Mg yr^{-1} over years 1–3), and from year 4 onward GT remains around ~ 5 Mg yr^{-1} (4.59–4.95 Mg yr^{-1} across scenarios). Cumulative totals (mean ± SD, Mg) increased from 345.6 ± 28.2 under RCP2.6 to 356.4 ± 25.9 under RCP4.5 and 368.3 ± 24.3 under RCP8.5. These values correspond to relative increases of +3.1% from RCP2.6 to RCP4.5, +6.6% from RCP2.6 to RCP8.5, and +3.3% from RCP4.5 to RCP8.5.

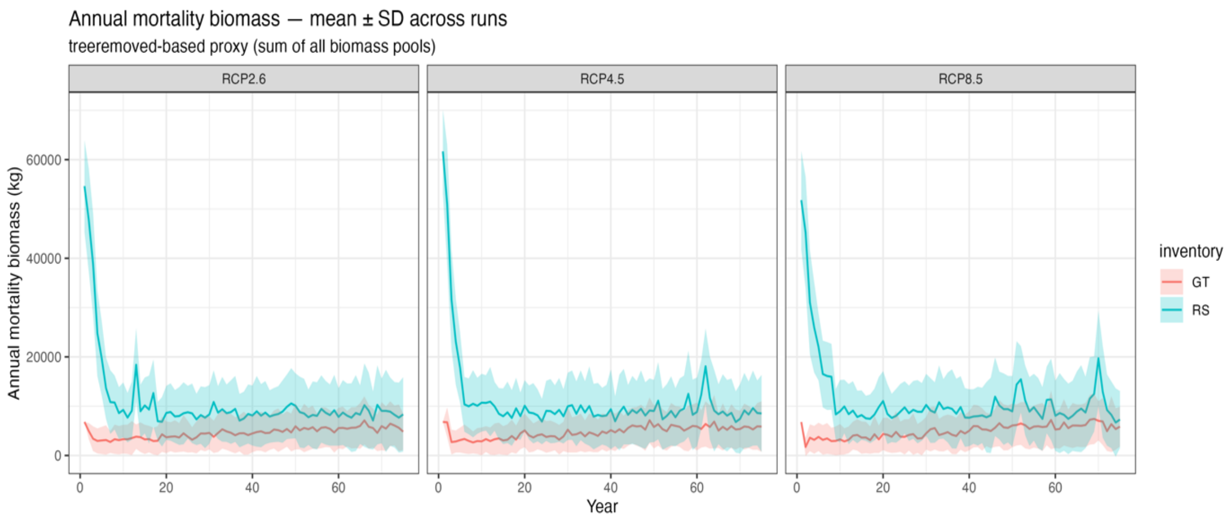

Figure 28 Annual mortality in kg per year for RS and GT across RCP2.6, RCP4.5, and RCP8.5. Lines show means of 100 runs and bands show ±SD.

Seasonal Productivity Dynamics

Seasonal productivity was quantified from the production_month table as monthly gross primary productivity (GPP; model units). For each simulation run, GPP values were aggregated to monthly means, and climatologies were derived across the 100 replicates per scenario. This approach captures both the timing of peak carbon uptake and the magnitude of seasonal fluxes.

Seasonal GPP dynamics

RS simulations showed clear seasonal differences among scenarios. In all cases, GPP rose from March and peaked in June–July, with RCP2.6 lowest, RCP4.5 intermediate, and RCP8.5 highest. Under RCP8.5, the post-peak decline was steeper, indicating stronger mid-summer heat and water stress. Seasonal means confirmed significant warming effects. In spring (MAM), GPP increased by ~4.3% (RCP4.5) and ~10.6% (RCP8.5) relative to RCP2.6; in summer (JJA), increases were ~4.6% and ~8.2%. ANOVA detected highly significant scenario effects ($p < 0.001$), with all pairwise contrasts significant. Warming thus enhanced spring productivity but intensified summer decline. GT simulations showed similar seasonal patterns but weaker sensitivity. Spring GPP rose by ~4.0% (RCP4.5) and ~9.7% (RCP8.5), and summer by ~4.3% and ~7.3%, respectively. Although scenario effects remained highly significant (p <

0.001), differences were consistently smaller than in RS, indicating a more buffered seasonal response.

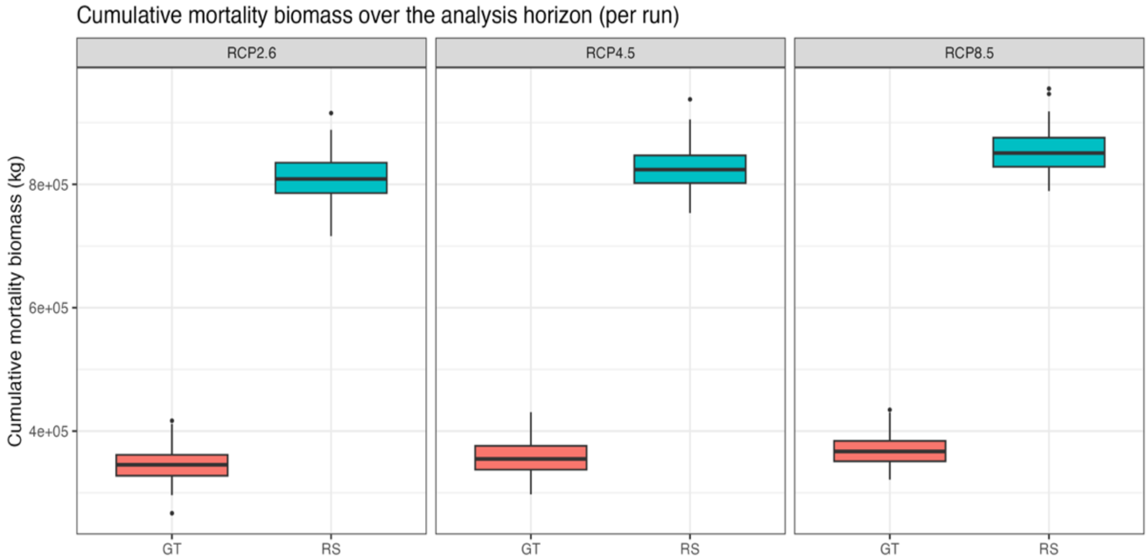

Figure 29 Cumulative mortality in kg per run for RS and GT across RCP2.6, RCP4.5, and RCP8.5. Boxplots summarize 100 runs.

Table 6 ANOVA results for across-scenario differences in seasonal GPP (MAM and JJA) under RS and GT initializations.

Season	Initialization	Effect	F-statistic	p-value
MAM	RS	RCP	8617.6	<0.001
MAM	GT	RCP	9050.5	<0.001
JJA	RS	RCP	1239.8	<0.001
JJA	GT	RCP	886.3	<0.001

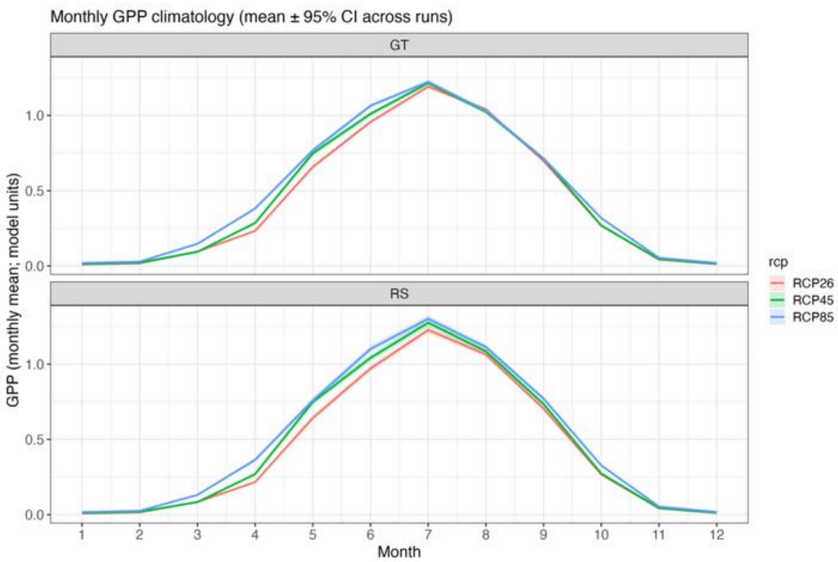

Figure 30 Monthly climatology of gross primary productivity (GPP; mean ± 95% CI across 100 runs) under RCP2.6, RCP4.5, and RCP8.5.

5 Discussion

The Mathislewald simulations demonstrate that climate forcing is the dominant driver of future growth, structure, mortality, and species composition in Central European montane forests. Moderate warming (RCP4.5) enhanced diameter and height increments as well as net primary productivity (NPP), whereas strong forcing (RCP8.5) initially stimulated growth but led to late-century declines in vitality. Although cumulative biomass was highest under RCP8.5 due to early growth gains and stock inertia (Pan et al. 2011; Pretzsch et al. 2014), this high-biomass state appears structurally fragile. The pattern reflects a non-linear balance between CO_2 fertilization (Norby and Zak 2011; Walker et al. 2021) and increasing heat and drought stress (Allen et al. 2010; McDowell et al. 2008), consistent with empirical evidence from the 2003 and 2018 droughts (Ciais et al. 2005; Schuldt et al. 2020).

Species composition shifted gradually but directionally. Norway spruce (*Picea abies*) declined across scenarios, while European beech (*Fagus sylvatica*) and silver fir (*Abies alba*) increased their relative shares, particularly under RCP8.5. This aligns with documented drought sensitivity of spruce and greater physiological plasticity of beech and fir (Hanewinkel et al. 2012; Vitali et al. 2017; Leuschner 2020). Shannon diversity increased with warming, mainly due to reduced spruce dominance, supporting findings that mixed stands enhance resilience (Pretzsch et al. 2013; Jactel et al. 2017). However, compositional change remained gradual, reflecting long tree lifespans and confirming that major turnover in temperate forests is slow without management intervention (Brang et al. 2014).

Structural development revealed important trade-offs. Warming promoted denser but shorter stands, reduced leaf area index (LAI), and elevated mortality. These patterns follow density–size relationships and self-thinning theory (Westoby 1984; Pretzsch 2009). Under RCP8.5, compressed canopy structure and rising mortality suggest increasing vulnerability to drought-related stress, even without disturbances. Because windthrow and bark beetle were excluded, mortality responses are likely conservative; disturbance risks are expected to intensify under warming, particularly in spruce-dominated systems (Seidl et al. 2017; Thom et al. 2017b; Hlásny et al. 2021).

Seasonally, climate change altered not only the magnitude but also the timing of productivity. Spring gross primary productivity (GPP) increased under warming due to earlier phenology (Menzel et al. 2006; Keenan et al. 2014), whereas summer productivity declined under RCP8.5, reflecting heightened drought stress. This redistribution mirrors observed drought-year dynamics in Europe (Ciais et al. 2005; Schwalm et al. 2010) and indicates increasing volatility of the carbon sink under strong forcing.

Methodological uncertainties affect magnitude but not direction of responses. Climate projections relied on a single downscaled GCM–RCM chain, and precipitation uncertainty remains substantial (Kotlarski et al. 2014). Model simplifications in iLand, including light-use efficiency formulations and simplified mortality processes (Seidl et al. 2012), may underestimate extreme drought impacts and overestimate CO_2 fertilization effects. Exclusion of disturbances further renders biomass projections conservative. Differences between remote sensing (RS) and ground-truth (GT) initialization affected absolute stocks but preserved identical scenario rankings, supporting the robustness of directional trends while highlighting the importance of inventory choice (Liang et al. 2016).

From a management perspective, the declining competitiveness of spruce and the increasing role of beech and fir suggest that diversification is essential for resilience (Bolte et al. 2009; Hanewinkel et al. 2012). Density regulation and promotion of mixed, structurally diverse stands can mitigate vulnerability to drought and disturbance (Pretzsch et al. 2017). Moderate forcing scenarios allow sustained productivity, whereas strong forcing leads to structurally crowded and potentially unstable systems despite high biomass.

Overall, the simulations indicate a bifurcated future: under moderate warming, montane forests may maintain productivity and gradually diversify; under strong forcing, they risk structural fragility, increased mortality, and unstable seasonal carbon dynamics. While absolute magnitudes remain uncertain, the directional signal is robust—climate change progressively weakens spruce dominance and reshapes Central European montane forests toward more mixed but stress-prone systems.

6 Conclusion

This research examined the future development of the Mathislewald forest under climate change using high-resolution remote sensing data and the process-based iLand model. Simulations from 2025 to 2100 under RCP2.6, RCP4.5, and RCP8.5 assessed growth, structure, species composition, mortality, and seasonal productivity, while comparing remote sensing (TLS) and ground-truth initializations to evaluate methodological robustness. Climate forcing emerged as the dominant driver of forest dynamics. Moderate warming (RCP4.5) sustained high growth and relatively stable productivity, whereas strong forcing (RCP8.5) initially stimulated growth but led to declining vitality, higher mortality, compressed canopy structure, and seasonal instability. Norway spruce consistently lost competitiveness, while beech and fir expanded, indicating a gradual shift toward more diverse and potentially resilient mixtures. Seasonal productivity shifted toward stronger spring uptake but greater summer vulnerability under high forcing. Although remote sensing initialization slightly underestimated absolute values, it reproduced identical climate-driven patterns, confirming its suitability for process-based modeling. These findings underline the risks of continued spruce dominance under warming and highlight the importance of diversification, density regulation, and promotion of mixed stands for climate adaptation. While moderate emission pathways allow forests to maintain productivity and structural stability, strong forcing leads to increasingly fragile systems despite high biomass stocks. Uncertainties remain due to the use of a single climate model chain, exclusion of disturbance processes, and model parameter assumptions. Nevertheless, the consistency of directional responses across scenarios and initialization datasets supports the robustness of the conclusions. Future research should incorporate disturbance regimes, management scenarios, multi-model climate ensembles, and further integration of remote sensing to enhance realism and scalability.

7 Acknowledgements

I would like to express my deepest gratitude to my supervisor, Dr. Julian Frey, for his invaluable guidance, support, and encouragement throughout the course of this thesis. His constructive feedback and expertise were essential in shaping both the scientific direction and the quality of this work. I am equally grateful to my second supervisor, Prof. Dr. René Orth, whose insights and advice greatly enriched this study. I would also like to sincerely thank Katja Kröner for her continuous support, patience, and countless helpful discussions that guided me through many stages of the research. My special thanks go to Jakob Albrecht, who generously shared data, provided crucial explanations, and assisted in clarifying methodological details that were fundamental for model initialization. I am also thankful to Jonas Kerber (TUM) for providing nitrogen data. I would like to express my sincere appreciation to the Forest Department of Myanmar for their encouragement and institutional support throughout my academic journey. Their commitment to forestry development and sustainable forest management has been a continuous source of inspiration for my professional aspirations.

I would also like to acknowledge Prof. Dr. Thomas Seifert for his support and leadership in making this joint degree program an inspiring academic journey at the University of Freiburg. My warm thanks go to Marjoriitta Möttönen, program coordinator at UEF, and to Prof. Timo Tokola, program director of MSc European Forestry, for their guidance and dedicated work in coordinating and supporting the program. Thereafter, my incredible gratitude goes to the MSc European Forestry-EMJMD scholarship program for supporting me financially throughout my two years abroad.

8 References

Abramowitz, Gab, Nadja Herger, Ethan Gutmann, et al. 2019. “ESD Reviews: Model Dependence in Multi-Model Climate Ensembles: Weighting, Sub-Selection and out-of-Sample Testing.” *Earth System Dynamics* 10 (1): 91–105. https://doi.org/10.5194/esd-10-91-2019.

Allen, Craig D., Alison K. Macalady, Haroun Chenchouni, et al. 2010. “A Global Overview of Drought and Heat-Induced Tree Mortality Reveals Emerging Climate Change Risks for Forests.” *Forest Ecology and Management* 259 (4): 660–84. https://doi.org/10.1016/j.foreco.2009.09.001.

Anderson, Ray G, Josep G Canadell, James T Randerson, et al. 2011. “Biophysical Considerations in Forestry for Climate Protection.” *Frontiers in Ecology and the Environment* 9 (3): 174–82. https://doi.org/10.1890/090179.

Bauhus, Jürgen, Peter van der Meer, and Markku Kanninen, eds. 2010. *Ecosystem Goods and Services from Plantation Forests*. The Earthscan Forest Library. Earthscan.

Beck, Hylke E., Niklaus E. Zimmermann, Tim R. McVicar, Noemi Vergopolan, Alexis Berg, and Eric F. Wood. 2018. “Present and Future Köppen-Geiger Climate Classification Maps at 1-Km Resolution.” *Scientific Data* 5 (1): 180214. https://doi.org/10.1038/sdata.2018.214.

BMEL, Federal Ministry of Food, Agriculture and Consumer Protection. 2020. *Forest Strategy 2020: Sustainable Forest Management – An Opportunity and a Challenge for Society*. Berlin, Germany. https://www.bmleh.de/SharedDocs/Downloads/EN/Publications/ForestStrategy2020.pdf?__blob=publicationFile&v=4.

Bohn, Friedrich J., Karin Frank, and Andreas Huth. 2014. “Of Climate and Its Resulting Tree Growth: Simulating the Productivity of Temperate Forests.” *Ecological Modelling* 278 (April): 9–17. https://doi.org/10.1016/j.ecolmodel.2014.01.021.

Bolte, A., T. Czajkowski, and T. Kompa. 2007. “The North-Eastern Distribution Range of European Beech a Review.” *Forestry* 80 (4): 413–29. https://doi.org/10.1093/forestry/cpm028.

Bolte, Andreas, Christian Ammer, Magnus Löf, et al. 2009. “Adaptive Forest Management in Central Europe: Climate Change Impacts, Strategies and Integrative Concept.” *Scandinavian Journal of Forest Research* 24 (6): 473–82. https://doi.org/10.1080/02827580903418224.

Bonan, Gordon B. 2008. “Forests and Climate Change: Forcings, Feedbacks, and the Climate Benefits of Forests.” *Science* 320 (5882): 1444–49. https://doi.org/10.1126/science.1155121.

Bowditch, Euan, Giovanni Santopuoli, Franz Binder, et al. 2020. “What Is Climate-Smart Forestry? A Definition from a Multinational Collaborative Process Focused on Mountain Regions of Europe.” *Ecosystem Services* 43 (June): 101113. https://doi.org/10.1016/j.ecoser.2020.101113.

Brang, P., P. Spathelf, J. B. Larsen, et al. 2014. “Suitability of Close-to-Nature Silviculture for Adapting Temperate European Forests to Climate Change.” *Forestry* 87 (4): 492–503. https://doi.org/10.1093/forestry/cpu018.

Bréda, Nathalie, Roland Huc, André Granier, and Erwin Dreyer. 2006. “Temperate Forest Trees and Stands under Severe Drought: A Review of Ecophysiological Responses, Adaptation Processes and Long-Term Consequences.” *Annals of Forest Science* 63 (6): 625–44. https://doi.org/10.1051/forest:2006042.

Breil, Marcus, Edouard L. Davin, and Diana Rechid. 2021. “What Determines the Sign of the Evapotranspiration Response to Afforestation in European Summer?” *Biogeosciences* 18 (4): 1499–510. https://doi.org/10.5194/bg-18-1499-2021.

Breil, Marcus, Vanessa K. M. Schneider, and Joaquim G. Pinto. 2024. “The Effect of Forest Cover Changes on the Regional Climate Conditions in Europe during the Period 1986–2015.” *Biogeosciences* 21 (3): 811–24. https://doi.org/10.5194/bg-21-811-2024.

Bugmann, Harald. 2001. “A Review of Forest Gap Models.” *Climatic Change* 51 (3–4): 259–305. https://doi.org/10.1023/A:1012525626267.

Bugmann, Harald, Rupert Seidl, Florian Hartig, et al. 2019. “Tree Mortality Submodels Drive Simulated Long-term Forest Dynamics: Assessing 15 Models from the Stand to Global Scale.” *Ecosphere* 10 (2). https://doi.org/10.1002/ecs2.2616.

Buras, Allan, Anja Rammig, and Christian S. Zang. 2020. “Quantifying Impacts of the 2018 Drought on European Ecosystems in Comparison to 2003.” *Biogeosciences* 17 (6): 1655–72. https://doi.org/10.5194/bg-17-1655-2020.

Bychkov, Igor, and Anastasia Popova. 2023. “Forest Landscape Model Initialization with Remotely Sensed-Based Open-Source Databases in the Absence of Inventory Data.” *Forests* 14 (10): 1995. https://doi.org/10.3390/f14101995.

Calders, Kim, Jennifer Adams, John Armston, et al. 2020. “Terrestrial Laser Scanning in Forest Ecology: Expanding the Horizon.” *Remote Sensing of Environment* 251 (December): 112102. https://doi.org/10.1016/j.rse.2020.112102.

Cannon, Alex J., Stephen R. Sobie, and Trevor Q. Murdock. 2015. “Bias Correction of GCM Precipitation by Quantile Mapping: How Well Do Methods Preserve Changes in Quantiles and Extremes?” *Journal of Climate* 28 (17): 6938–59. https://doi.org/10.1175/JCLI-D-14-00754.1.

Ciais, Ph., M. Reichstein, N. Viovy, et al. 2005. “Europe-Wide Reduction in Primary Productivity Caused by the Heat and Drought in 2003.” *Nature* 437 (7058): 529–33. https://doi.org/10.1038/nature03972.

Coops, Nicholas C., Piotr Tompalski, Tristan R.H. Goodbody, et al. 2021. “Modelling Lidar-Derived Estimates of Forest Attributes over Space and Time: A Review of Approaches and Future Trends.” *Remote Sensing of Environment* 260 (July): 112477. https://doi.org/10.1016/j.rse.2021.112477.

Coppola, Erika, Rita Nogherotto, James M. Ciarlo’, et al. 2021. “Assessment of the European Climate Projections as Simulated by the Large EURO-CORDEX Regional and Global Climate Model Ensemble.” *Journal of Geophysical Research: Atmospheres* 126 (4): e2019JD032356. https://doi.org/10.1029/2019JD032356.

Dalponte, Michele, and David A. Coomes. 2016. “Tree-centric Mapping of Forest Carbon Density from Airborne Laser Scanning and Hyperspectral Data.” *Methods in Ecology and Evolution* 7 (10): 1236–45. https://doi.org/10.1111/2041-210X.12575.

Dittmar, Christoph, Wolfgang Zech, and Wolfram Elling. 2003. “Growth Variations of Common Beech (Fagus Sylvatica L.) under Different Climatic and Environmental Conditions in Europe—a Dendroecological Study.” *Forest Ecology and Management* 173 (1–3): 63–78. https://doi.org/10.1016/S0378-1127(01)00816-7.

Dobbertin, Matthias. 2005. “Tree Growth as Indicator of Tree Vitality and of Tree Reaction to Environmental Stress: A Review.” *European Journal of Forest Research* 124 (4): 319–33. https://doi.org/10.1007/s10342-005-0085-3.

Dollinger, Christina, Werner Rammer, Kureha F. Suzuki, et al. 2024. “Beyond Resilience: Responses to Changing Climate and Disturbance Regimes in Temperate Forest Landscapes across the Northern Hemisphere.” *Global Change Biology* 30 (8): e17468. https://doi.org/10.1111/gcb.17468.

DWD, Deutscher Wetterdienst (German Weather Service). 2025. “Climate at Selected Weather Stations in Baden-Württemberg.” Our Services – Climate at Selected Weather Stations in Baden-Württemberg. https://www.dwd.de/EN/ourservices/cos/baden-wuerttenberg.html.

Ehbrecht, Martin, Dominik Seidel, Peter Annighöfer, et al. 2021. “Global Patterns and Climatic Controls of Forest Structural Complexity.” *Nature Communications* 12 (1). https://doi.org/10.1038/s41467-020-20767-z.

Fassnacht, Fabian Ewald, Hooman Latifi, Krzysztof Stereńczak, et al. 2016. “Review of Studies on Tree Species Classification from Remotely Sensed Data.” *Remote Sensing of Environment* 186 (December): 64–87. https://doi.org/10.1016/j.rse.2016.08.013.

Fernández-Martínez, M., J. Sardans, F. Chevallier, et al. 2019. “Global Trends in Carbon Sinks and Their Relationships with CO2 and Temperature.” *Nature Climate Change* 9 (1): 73–79. https://doi.org/10.1038/s41558-018-0367-7.

Fischer, Rico, Friedrich Bohn, Mateus Dantas De Paula, et al. 2016a. “Lessons Learned from Applying a Forest Gap Model to Understand Ecosystem and Carbon Dynamics of Complex Tropical Forests.” *Ecological Modelling* 326 (April): 124–33. https://doi.org/10.1016/j.ecolmodel.2015.11.018.

Fischer, Rico, Friedrich Bohn, Mateus Dantas De Paula, et al. 2016b. “Lessons Learned from Applying a Forest Gap Model to Understand Ecosystem and Carbon Dynamics of Complex Tropical Forests.” *Ecological Modelling* 326 (April): 124–33. https://doi.org/10.1016/j.ecolmodel.2015.11.018.

Fisher, Rosie A., Charles D. Koven, William R. L. Anderegg, et al. 2018. “Vegetation Demographics in Earth System Models: A Review of Progress and Priorities.” *Global Change Biology* 24 (1): 35–54. https://doi.org/10.1111/gcb.13910.

Frey, Julian, and Zoe Schindler. 2024a. *JulFrey/CspStandSegmentation: Single Tree Segmentation from Terestrial LiDAR Forest Scans*. V. v1.1.0. Zenodo, released November 22. https://doi.org/10.5281/ZENODO.14204459.

Frey, Julian, and Zoe Schindler. 2024b. *JulFrey/DetailView: DetailView Model for Tree Species Classification Based on Single Tree LiDAR Data*. V. v1.0.0. Zenodo, released November 22. https://doi.org/10.5281/ZENODO.14204431.

Giorgi, Filippo, Colin Jones, and Ghassem R Asrar. 2009. *Addressing Climate Information Needs at the Regional Level: The CORDEX Framework*.

Global Forest Resources Assessment 2020. 2020. FAO. https://doi.org/10.4060/ca9825en.

Hanewinkel, Marc, Dominik A. Cullmann, Mart-Jan Schelhaas, Gert-Jan Nabuurs, and Niklaus E. Zimmermann. 2012. “Climate Change May Cause Severe Loss in the Economic Value of European Forest Land.” *Nature Climate Change* 3 (3): 203–7. https://doi.org/10.1038/nclimate1687.

Hari, Vittal, Oldrich Rakovec, Yannis Markonis, Martin Hanel, and Rohini Kumar. 2020. “Increased Future Occurrences of the Exceptional 2018–2019 Central European Drought under Global Warming.” *Scientific Reports* 10 (1): 12207. https://doi.org/10.1038/s41598-020-68872-9.

Hartmann, Henrik, Henry D. Adams, William M. Hammond, et al. 2018. “Identifying Differences in Carbohydrate Dynamics of Seedlings and Mature Trees to Improve Carbon Allocation in Models for Trees and Forests.” *Environmental and Experimental Botany* 152 (August): 7–18. https://doi.org/10.1016/j.envexpbot.2018.03.011.

Hartmann, Peter, Moritz Niethammer, Raphael Habel, Dietmar Zirlewagen, and Heike Puhlmann. 2024. “Regionalization of soil data for forest areas in Baden-Württemberg.” *standort.wald – Mitteilungen des Vereins für Standortskunde und Vegetationskunde* 53 (December): 69–93.

Hartung, Carl, Adam Lerer, Yaw Anokwa, Clint Tseng, Waylon Brunette, and Gaetano Borriello. 2010. “Open Data Kit: Tools to Build Information Services for Developing Regions.” *Proceedings of the 4th ACM/IEEE International Conference on Information and Communication Technologies and Development*, December 13, 1–12. https://doi.org/10.1145/2369220.2369236.

Heisner, Ute, Bernd Raber, and Ernst E. Hildebrand. 2004. “The Importance of the Soil Skeleton for Plant-Available Nutrients in Sites of the Southern Black Forest, Germany.” *European Journal of Forest Research* 123 (4): 249–57. https://doi.org/10.1007/s10342-004-0041-7.

Hlásny, Tomáš, Louis König, Paal Krokene, et al. 2021. “Bark Beetle Outbreaks in Europe: State of Knowledge and Ways Forward for Management.” *Current Forestry Reports* 7 (3): 138–65. https://doi.org/10.1007/s40725-021-00142-x.

Hlásny, Tomáš, Csaba Mátyás, Rupert Seidl, et al. 2014. “Climate Change Increases the Drought Risk in Central European Forests: What Are the Options for Adaptation?” *Forestry Journal* 60 (1): 5–18. https://doi.org/10.2478/forj-2014-0001.

Huth, A, and T Ditzer. 2001. “Long-Term Impacts of Logging in a Tropical Rain Forest — a Simulation Study.” *Forest Ecology and Management* 142 (1–3): 33–51. https://doi.org/10.1016/S0378-1127(00)00338-8.

Huth, Radan, Christoph Beck, Andreas Philipp, et al. 2008. “Classifications of Atmospheric Circulation Patterns: Recent Advances and Applications.” *Annals of the New York Academy of Sciences* 1146 (1): 105–52. https://doi.org/10.1196/annals.1446.019.

Iland Documentation. 2025. “Spin-Up.” https://iland-model.org/spinup.

Immitzer, Markus, Clement Atzberger, and Tatjana Koukal. 2012. “Tree Species Classification with Random Forest Using Very High Spatial Resolution 8-Band WorldView-2 Satellite Data.” *Remote Sensing* 4 (9): 2661–93. https://doi.org/10.3390/rs4092661.

Intergovernmental Panel On Climate Change (IPCC). 2023. *Climate Change 2021 – The Physical Science Basis: Working Group I Contribution to the Sixth Assessment Report of the Intergovernmental Panel on Climate Change*. 1st ed. Cambridge University Press. https://doi.org/10.1017/9781009157896.

IPCC, ed. 2014. *Climate Change 2014: Synthesis Report. Contribution of Working Groups I, II and III to the Fifth Assessment Report of the Intergovernmental Panel on Climate Change*. Intergovernmental Panel on Climate Change. https://www.ipcc.ch/report/ar5/syr/.

Ishii, Hiroaki T., Shin-ichi Tanabe, and Tsutom Hiura. 2004. “Exploring the Relationships Among Canopy Structure, Stand Productivity, and Biodiversity of Temperate Forest Ecosystems.” *Forest Science* 50 (3): 342–55. https://doi.org/10.1093/forestscience/50.3.342.

Jacob, Daniela, Juliane Petersen, Bastian Eggert, et al. 2014. “EURO-CORDEX: New High-Resolution Climate Change Projections for European Impact Research.” *Regional Environmental Change* 14 (2): 563–78. https://doi.org/10.1007/s10113-013-0499-2.

Jactel, Hervé, Jürgen Bauhus, Johanna Boberg, et al. 2017. “Tree Diversity Drives Forest Stand Resistance to Natural Disturbances.” *Current Forestry Reports* 3 (3): 223–43. https://doi.org/10.1007/s40725-017-0064-1.

Kauppi, Pekka E., Maximilian Posch, and Pentti Pirinen. 2014. “Large Impacts of Climatic Warming on Growth of Boreal Forests since 1960.” *PLoS ONE* 9 (11): e111340. https://doi.org/10.1371/journal.pone.0111340.

Keenan, Trevor F., Josh Gray, Mark A. Friedl, et al. 2014. “Net Carbon Uptake Has Increased through Warming-Induced Changes in Temperate Forest Phenology.” *Nature Climate Change* 4 (7): 598–604. https://doi.org/10.1038/nclimate2253.

Kjellström, Erik, Grigory Nikulin, Gustav Strandberg, et al. 2018. “European Climate Change at Global Mean Temperature Increases of 1.5 and 2 °C above Pre-Industrial Conditions as Simulated by the EURO-CORDEX Regional Climate Models.” *Earth System Dynamics* 9 (2): 459–78. https://doi.org/10.5194/esd-9-459-2018.

Klopcic, Matija, Ales Poljanec, and Andrej Boncina. 2012. “Modelling Natural Recruitment of European Beech (Fagus Sylvatica L.).” *Forest Ecology and Management* 284 (November): 142–51. https://doi.org/10.1016/j.foreco.2012.07.049.

Kotlarski, S., K. Keuler, O. B. Christensen, et al. 2014. "Regional Climate Modeling on European Scales: A Joint Standard Evaluation of the EURO-CORDEX RCM Ensemble." *Geoscientific Model Development* 7 (4): 1297–333. https://doi.org/10.5194/gmd-7-1297-2014.

Landsberg, J.J., and R.H. Waring. 1997. "A Generalised Model of Forest Productivity Using Simplified Concepts of Radiation-Use Efficiency, Carbon Balance and Partitioning." *Forest Ecology and Management* 95 (3): 209–28. https://doi.org/10.1016/S0378-1127(97)00026-1.

Larysch, Elena, Julian Frey, Zoe Schindler, et al. 2025. "Quantifying and Mapping the Ready-to-Use Veneer Volume of European Beech Trees Based on Terrestrial Laser Scanning Data." *European Journal of Forest Research*, ahead of print, June 23. https://doi.org/10.1007/s10342-025-01796-z.

Le Quéré, Corinne, Robbie M. Andrew, Pierre Friedlingstein, et al. 2018. "Global Carbon Budget 2018." *Earth System Science Data* 10 (4): 2141–94. https://doi.org/10.5194/essd-10-2141-2018.

Leuschner, Christoph. 2020. "Drought Response of European Beech (Fagus Sylvatica L.)—A Review." *Perspectives in Plant Ecology, Evolution and Systematics* 47 (December): 125576. https://doi.org/10.1016/j.ppees.2020.125576.

Leuschner, Christoph, and Heinz Ellenberg. 2017. *Ecology of Central European Forests: Vegetation Ecology of Central Europe, Volume I*. Springer International Publishing. https://doi.org/10.1007/978-3-319-43042-3.

Li, Wenkai, Qinghua Guo, Marek K. Jakubowski, and Maggi Kelly. 2012. "A New Method for Segmenting Individual Trees from the Lidar Point Cloud." *Photogrammetric Engineering & Remote Sensing* 78 (1): 75–84. https://doi.org/10.14358/PERS.78.1.75.

Liang, Xinlian, Ville Kankare, Juha Hyyppä, et al. 2016. "Terrestrial Laser Scanning in Forest Inventories." *ISPRS Journal of Photogrammetry and Remote Sensing* 115 (May): 63–77. https://doi.org/10.1016/j.isprsjprs.2016.01.006.

Lindner, Marcus, Michael Maroschek, Sigrid Netherer, et al. 2010a. "Climate Change Impacts, Adaptive Capacity, and Vulnerability of European Forest Ecosystems." *Forest Ecology and Management* 259 (4): 698–709. https://doi.org/10.1016/j.foreco.2009.09.023.

Lindner, Marcus, Michael Maroschek, Sigrid Netherer, et al. 2010b. "Climate Change Impacts, Adaptive Capacity, and Vulnerability of European Forest Ecosystems." *Forest Ecology and Management* 259 (4): 698–709. https://doi.org/10.1016/j.foreco.2009.09.023.

Makela, A., J. Landsberg, A. R. Ek, et al. 2000. "Process-Based Models for Forest Ecosystem Management: Current State of the Art and Challenges for Practical Implementation." *Tree Physiology* 20 (5–6): 289–98. https://doi.org/10.1093/treephys/20.5-6.289.

Martinez Del Castillo, Edurne, Christian S. Zang, Allan Buras, et al. 2022. "Climate-Change-Driven Growth Decline of European Beech Forests." *Communications Biology* 5 (1): 163. https://doi.org/10.1038/s42003-022-03107-3.

Marzini, Sebastian, Erich Tasser, Camilla Wellstein, Katharina Albrich, Werner Rammer, and Marco Mina. 2025. "Future Expansion of Upper Forest-Grassland Ecotone under Land-Use and Climate Change in the Eastern Alps." *Landscape Ecology* 40 (3): 55. https://doi.org/10.1007/s10980-025-02070-8.

McDowell, Nate, William T. Pockman, Craig D. Allen, et al. 2008. "Mechanisms of Plant Survival and Mortality during Drought: Why Do Some Plants Survive While Others Succumb to Drought?" *New Phytologist* 178 (4): 719–39. https://doi.org/10.1111/j.1469-8137.2008.02436.x.

Meesenburg, Henning, Winfried Riek, Bernd Ahrends, et al. 2019. "Soil Acidification in German Forest Soils." In *Status and Dynamics of Forests in Germany*, edited by Nicole Wellbrock and Andreas Bolte, vol. 237. Ecological Studies. Springer International Publishing. https://doi.org/10.1007/978-3-030-15734-0_4.

Menzel, Annette, Tim H. Sparks, Nicole Estrella, et al. 2006. "European Phenological Response to Climate Change Matches the Warming Pattern." *Global Change Biology* 12 (10): 1969–76. https://doi.org/10.1111/j.1365-2486.2006.01193.x.

Messier, Christian, Jürgen Bauhus, Rita Sousa-Silva, et al. 2021. "For the Sake of Resilience and Multifunctionality, Let's Diversify Planted Forests!" *Conservation Letters* 15 (1): e12829. https://doi.org/10.1111/conl.12829.

Mina, Marco, Sebastian Marzini, Alice Crespi, and Katharina Albrich. 2025. "Building Virtual Forest Landscapes to Support Forest Management: The Challenge of Parameterization." *Forests Monitor* 2 (1): 49–96. https://doi.org/10.62320/fm.v2i1.19.

Morales, Pablo, Thomas Hickler, David P. Rowell, Benjamin Smith, and Martin T. Sykes. 2007. "Changes in European Ecosystem Productivity and Carbon Balance Driven by Regional Climate Model Output." *Global Change Biology* 13 (1): 108–22. https://doi.org/10.1111/j.1365-2486.2006.01289.x.

Morin, Xavier, Lorenz Fahse, Hervé Jactel, Michael Scherer-Lorenzen, Raúl García-Valdés, and Harald Bugmann. 2018. "Long-Term Response of Forest Productivity to Climate Change Is Mostly Driven by Change in Tree Species Composition." *Scientific Reports* 8 (1). https://doi.org/10.1038/s41598-018-23763-y.

Moss, Richard H., Jae A. Edmonds, Kathy A. Hibbard, et al. 2010. "The next Generation of Scenarios for Climate Change Research and Assessment." *Nature* 463 (7282): 747–56. https://doi.org/10.1038/nature08823.

Nabuurs, Gert-Jan, Marcus Lindner, Pieter J. Verkerk, et al. 2013. "First Signs of Carbon Sink Saturation in European Forest Biomass." *Nature Climate Change* 3 (9): 792–96. https://doi.org/10.1038/nclimate1853.

Nabuurs, Gert-Jan, Pieter Johannes Verkerk, and Mart-Jan Schelhaas. 2018. *Climate-Smart Forestry: Mitigation Impacts in Three European Regions*. With European Forest Institute. From Science to Policy / European Forest Institute 6. EFI.

Naudts, Kim, Yiying Chen, Matthew J. McGrath, et al. 2016. "Europe's Forest Management Did Not Mitigate Climate Warming." *Science* 351 (6273): 597–600. https://doi.org/10.1126/science.aad7270.

Norby, Richard J., and Donald R. Zak. 2011. "Ecological Lessons from Free-Air CO_2 Enrichment (FACE) Experiments." *Annual Review of Ecology, Evolution, and Systematics* 42 (1): 181–203. https://doi.org/10.1146/annurev-ecolsys-102209-144647.

O'Neill, Brian C., Elmar Kriegler, Kristie L. Ebi, et al. 2017. "The Roads Ahead: Narratives for Shared Socioeconomic Pathways Describing World Futures in the 21st Century." *Global Environmental Change* 42 (January): 169–80. https://doi.org/10.1016/j.gloenvcha.2015.01.004.

Pan, Yude, Richard A. Birdsey, Jingyun Fang, et al. 2011. "A Large and Persistent Carbon Sink in the World's Forests." *Science* 333 (6045): 988–93. https://doi.org/10.1126/science.1201609.

Pranindita, Agnes, Lan Wang-Erlandsson, Ingo Fetzer, and Adriaan J. Teuling. 2022. "Moisture Recycling and the Potential Role of Forests as Moisture Source during European Heatwaves." *Climate Dynamics* 58 (1–2): 609–24. https://doi.org/10.1007/s00382-021-05921-7.

Pretzsch, H., G. Schütze, and E. Uhl. 2013. "Resistance of European Tree Species to Drought Stress in Mixed *versus* Pure Forests: Evidence of Stress Release by Inter-specific Facilitation." *Plant Biology* 15 (3): 483–95. https://doi.org/10.1111/j.1438-8677.2012.00670.x.

Pretzsch, Hans. 2009. *Forest Dynamics, Growth and Yield: From Measurement to Model*. Springer Berlin Heidelberg. https://doi.org/10.1007/978-3-540-88307-4.

Pretzsch, Hans, Peter Biber, Gerhard Schütze, Enno Uhl, and Thomas Rötzer. 2014. "Forest Stand Growth Dynamics in Central Europe Have Accelerated since 1870." *Nature Communications* 5 (1). https://doi.org/10.1038/ncomms5967.

Pretzsch, Hans, David I. Forrester, and Jürgen Bauhus, eds. 2017. *Mixed-Species Forests*. Springer Berlin Heidelberg. https://doi.org/10.1007/978-3-662-54553-9.

Pretzsch, Hans, Gerhard Schütze, and Peter Biber. 2018. "Drought Can Favour the Growth of Small in Relation to Tall Trees in Mature Stands of Norway Spruce and European Beech." *Forest Ecosystems* 5 (1). https://doi.org/10.1186/s40663-018-0139-x.

Prietzel, Jörg. 2001. "Arylsulfatase Activities in Soils of the Black Forest/Germany—Seasonal Variation and Effect of (NH4)2SO4 Fertilization." *Soil Biology and Biochemistry* 33 (10): 1317–28. https://doi.org/10.1016/S0038-0717(01)00037-2.

Prietzel, Jörg, Lothar Zimmermann, Alfred Schubert, and Dominik Christophel. 2016. "Organic Matter Losses in German Alps Forest Soils since the 1970s Most Likely Caused by Warming." *Nature Geoscience* 9 (7): 543–48. https://doi.org/10.1038/ngeo2732.

Puliti, Stefano, Emily R. Lines, Jana Müllerová, et al. 2025. "Benchmarking Tree Species Classification from Proximally Sensed Laser Scanning Data: Introducing the FOR-SPECIES20K Dataset." *Methods in Ecology and Evolution* 16 (4): 801–18. https://doi.org/10.1111/2041-210x.14503.

Rammer, Werner, and Rupert Seidl. 2015. "Coupling Human and Natural Systems: Simulating Adaptive Management Agents in Dynamically Changing Forest Landscapes." *Global Environmental Change* 35 (November): 475–85. https://doi.org/10.1016/j.gloenvcha.2015.10.003.

Rammer, Werner, Dominik Thom, Martin Baumann, et al. 2024. "The Individual-Based Forest Landscape and Disturbance Model iLand: Overview, Progress, and Outlook." *Ecological Modelling* 495 (September): 110785. https://doi.org/10.1016/j.ecolmodel.2024.110785.

Reyer, Christopher P O, Stephen Bathgate, Kristina Blennow, et al. 2017. "Are Forest Disturbances Amplifying or Canceling out Climate Change-Induced Productivity Changes in European Forests?" *Environmental Research Letters* 12 (3): 034027. https://doi.org/10.1088/1748-9326/aa5ef1.

Reyer, Christopher P. O., Niels Brouwers, Anja Rammig, et al. 2015. "Forest Resilience and Tipping Points at Different Spatio-temporal Scales: Approaches and Challenges." *Journal of Ecology* 103 (1): 5–15. https://doi.org/10.1111/1365-2745.12337.

Reyer, Christopher P. O., Ramiro Silveyra Gonzalez, Klara Dolos, et al. 2020. "The PROFOUND Database for Evaluating Vegetation Models and Simulating Climate Impacts on European Forests." *Earth System Science Data* 12 (2): 1295–320. https://doi.org/10.5194/essd-12-1295-2020.

Running, Steven W., and E. Raymond Hunt. 1993. "Generalization of a Forest Ecosystem Process Model for Other Biomes, BIOME-BGC, and an Application for Global-Scale Models." In *Scaling Physiological Processes*. Elsevier. https://doi.org/10.1016/B978-0-12-233440-5.50014-2.

Schindler, Zoe, and Julian Frey. 2024. *Training Weights to Classify Tree Species from Single Tree LiDAR Point Clouds - the DetailView AI-Model.* FreiData, released October 28. https://doi.org/10.60493/F850A-BB152.

Schneider, Fabian D., Felix Morsdorf, Bernhard Schmid, et al. 2017. "Mapping Functional Diversity from Remotely Sensed Morphological and Physiological Forest Traits." *Nature Communications* 8 (1): 1441. https://doi.org/10.1038/s41467-017-01530-3.

Schuldt, Bernhard, Allan Buras, Matthias Arend, et al. 2020. "A First Assessment of the Impact of the Extreme 2018 Summer Drought on Central European Forests." *Basic and Applied Ecology* 45 (June): 86–103. https://doi.org/10.1016/j.baae.2020.04.003.

Schwalm, Christopher R., Christopher A. Williams, Kevin Schaefer, et al. 2010. "Assimilation Exceeds Respiration Sensitivity to Drought: A FLUXNET Synthesis." *Global Change Biology* 16 (2): 657–70. https://doi.org/10.1111/j.1365-2486.2009.01991.x.

Seidl, Rupert, Werner Rammer, Robert M. Scheller, and Thomas A. Spies. 2012. "An Individual-Based Process Model to Simulate Landscape-Scale Forest Ecosystem Dynamics." *Ecological Modelling* 231 (April): 87–100. https://doi.org/10.1016/j.ecolmodel.2012.02.015.

Seidl, Rupert, Mart-Jan Schelhaas, Werner Rammer, and Pieter Johannes Verkerk. 2014. "Increasing Forest Disturbances in Europe and Their Impact on Carbon Storage." *Nature Climate Change* 4 (9): 806–10. https://doi.org/10.1038/nclimate2318.

Seidl, Rupert, Dominik Thom, Markus Kautz, et al. 2017. "Forest Disturbances under Climate Change." *Nature Climate Change* 7 (6): 395–402. https://doi.org/10.1038/nclimate3303.

Senf, Cornelius, Dirk Pflugmacher, Yang Zhiqiang, et al. 2018. "Canopy Mortality Has Doubled in Europe's Temperate Forests over the Last Three Decades." *Nature Communications* 9 (1): 4978. https://doi.org/10.1038/s41467-018-07539-6.

Senf, Cornelius, and Rupert Seidl. 2020. "Mapping the Forest Disturbance Regimes of Europe." *Nature Sustainability* 4 (1): 63–70. https://doi.org/10.1038/s41893-020-00609-y.

Spiecker, Heinrich. 2003. "Silvicultural Management in Maintaining Biodiversity and Resistance of Forests in Europe—Temperate Zone." *Journal of Environmental Management* 67 (1): 55–65. https://doi.org/10.1016/s0301-4797(02)00188-3.

Spinoni, J., G. Naumann, and J. Vogt. 2015. "Spatial Patterns of European Droughts under a Moderate Emission Scenario." *Advances in Science and Research* 12 (1): 179–86. https://doi.org/10.5194/asr-12-179-2015.

Tebaldi, Claudia, and Reto Knutti. 2007. "The Use of the Multi-Model Ensemble in Probabilistic Climate Projections." *Philosophical Transactions of the Royal Society A: Mathematical, Physical and Engineering Sciences* 365 (1857): 2053–75. https://doi.org/10.1098/rsta.2007.2076.

Temperli, Christian, Harald Bugmann, and Ché Elkin. 2013. "Cross-scale Interactions among Bark Beetles, Climate Change, and Wind Disturbances: A Landscape Modeling Approach." *Ecological Monographs* 83 (3): 383–402. https://doi.org/10.1890/12-1503.1.

Temperli, Christian, Jürgen Zell, Harald Bugmann, and Ché Elkin. 2013. "Sensitivity of Ecosystem Goods and Services Projections of a Forest Landscape Model to Initialization Data." *Landscape Ecology* 28 (7): 1337–52. https://doi.org/10.1007/s10980-013-9882-0.

Themeßl, Matthias Jakob, Andreas Gobiet, and Georg Heinrich. 2012. "Empirical-Statistical Downscaling and Error Correction of Regional Climate Models and Its Impact on the Climate Change Signal." *Climatic Change* 112 (2): 449–68. https://doi.org/10.1007/s10584-011-0224-4.

Thom, Dominik. 2024. "iLand Species Parameters." With Werner Rammer, Katharina Albrich, Kristin Braziunas, et al. Mendeley Data, June 4. https://doi.org/10.17632/58XDBWSKP8.1.

Thom, Dominik, Marina Golivets, Laura Edling, et al. 2019. "The Climate Sensitivity of Carbon, Timber, and Species Richness Covaries with Forest Age in Boreal–Temperate North America." *Global Change Biology* 25 (7): 2446–58. https://doi.org/10.1111/gcb.14656.

Thom, Dominik, Werner Rammer, Katharina Albrich, et al. 2024. "Parameters of 150 Temperate and Boreal Tree Species and Provenances for an Individual-Based Forest

Landscape and Disturbance Model." *Data in Brief* 55 (August): 110662. https://doi.org/10.1016/j.dib.2024.110662.

Thom, Dominik, Werner Rammer, and Rupert Seidl. 2017a. "Disturbances Catalyze the Adaptation of Forest Ecosystems to Changing Climate Conditions." *Global Change Biology* 23 (1): 269–82. https://doi.org/10.1111/gcb.13506.

Thom, Dominik, Werner Rammer, and Rupert Seidl. 2017b. "The Impact of Future Forest Dynamics on Climate: Interactive Effects of Changing Vegetation and Disturbance Regimes." *Ecological Monographs* 87 (4): 665–84. https://doi.org/10.1002/ecm.1272.

Thom, Dominik, and Rupert Seidl. 2016. "Natural Disturbance Impacts on Ecosystem Services and Biodiversity in Temperate and Boreal Forests." *Biological Reviews* 91 (3): 760–81. https://doi.org/10.1111/brv.12193.

Thornton, P.E, B.E Law, Henry L Gholz, et al. 2002. "Modeling and Measuring the Effects of Disturbance History and Climate on Carbon and Water Budgets in Evergreen Needleleaf Forests." *Agricultural and Forest Meteorology* 113 (1–4): 185–222. https://doi.org/10.1016/S0168-1923(02)00108-9.

Vitali, Valentina, Ulf Büntgen, and Jürgen Bauhus. 2017. "Silver Fir and Douglas Fir Are More Tolerant to Extreme Droughts than Norway Spruce in South-western Germany." *Global Change Biology* 23 (12): 5108–19. https://doi.org/10.1111/gcb.13774.

Vitasse, Yann, Alessandra Bottero, Martine Rebetez, et al. 2019. "What Is the Potential of Silver Fir to Thrive under Warmer and Drier Climate?" *European Journal of Forest Research* 138 (4): 547–60. https://doi.org/10.1007/s10342-019-01192-4.

Vitasse, Yann, Sylvain Delzon, Eric Dufrêne, et al. 2009. "Leaf Phenology Sensitivity to Temperature in European Trees: Do within-Species Populations Exhibit Similar Responses?" *Agricultural and Forest Meteorology* 149 (5): 735–44. https://doi.org/10.1016/j.agrformet.2008.10.019.

Vuuren, Detlef P. van, Jae Edmonds, Mikiko Kainuma, et al. 2011. "The Representative Concentration Pathways: An Overview." *Climatic Change* 109 (1): 5. https://doi.org/10.1007/s10584-011-0148-z.

Walker, Anthony P., Martin G. De Kauwe, Ana Bastos, et al. 2021. "Integrating the Evidence for a Terrestrial Carbon Sink Caused by Increasing Atmospheric CO_2." *New Phytologist* 229 (5): 2413–45. https://doi.org/10.1111/nph.16866.

Westoby, Mark. 1984. "The Self-Thinning Rule." In *Advances in Ecological Research*, vol. 14. Elsevier. https://doi.org/10.1016/S0065-2504(08)60171-3.

Wolf, Sebastian, Trevor F. Keenan, Joshua B. Fisher, et al. 2016. "Warm Spring Reduced Carbon Cycle Impact of the 2012 US Summer Drought." *Proceedings of the National Academy of Sciences* 113 (21): 5880–85. https://doi.org/10.1073/pnas.1519620113.

Wolfe, Brett T., John S. Sperry, and Thomas A. Kursar. 2016. "Does Leaf Shedding Protect Stems from Cavitation during Seasonal Droughts? A Test of the Hydraulic Fuse Hypothesis." *New Phytologist* 212 (4): 1007–18. https://doi.org/10.1111/nph.14087.

Xiang, Binbin, Maciej Wielgosz, Theodora Kontogianni, et al. 2024. "Automated Forest Inventory: Analysis of High-Density Airborne LiDAR Point Clouds with 3D Deep Learning." *Remote Sensing of Environment* 305 (May): 114078. https://doi.org/10.1016/j.rse.2024.114078.

Yousefpour, Rasoul, Jette Bredahl Jacobsen, Bo Jellesmark Thorsen, Henrik Meilby, Marc Hanewinkel, and Karoline Oehler. 2012. "A Review of Decision-Making Approaches to Handle Uncertainty and Risk in Adaptive Forest Management under Climate Change." *Annals of Forest Science* 69 (1): 1–15. https://doi.org/10.1007/s13595-011-0153-4.

Yousefpour, Rasoul, Christian Temperli, Jette Bredahl Jacobsen, et al. 2017. "A Framework for Modeling Adaptive Forest Management and Decision Making under Climate Change." *Ecology and Society* 22 (4). https://doi.org/10.5751/es-09614-220440.

Yuan, Minshu, Qiuan Zhu, Jiang Zhang, et al. 2021. “Global Response of Terrestrial Gross Primary Productivity to Climate Extremes.” *Science of The Total Environment* 750 (January): 142337. https://doi.org/10.1016/j.scitotenv.2020.142337.

Zscheischler, Jakob, Seth Westra, Bart J. J. M. Van Den Hurk, et al. 2018. “Future Climate Risk from Compound Events.” *Nature Climate Change* 8 (6): 469–77. https://doi.org/10.1038/s41558-018-0156-3.